Quaternary Science Reviews 350 (2025) 109027

Contents lists available at ScienceDirect

Quaternary Science Reviews

journal homepage: www.elsevier.com/locate/quascirev

Glacial geology of the Hudson Mountains, Amundsen Sea sector, West Antarctica

Joanne S. Johnson [a,*], Keir A. Nichols [b], Teal R. Riley [a], Ryan A. Venturelli [c], Dominic A. Hodgson [a], Greg Balco [d,e], Brenda Hall [f], James A. Smith [a], John Woodward [g]

[a] British Antarctic Survey, High Cross, Madingley Road, Cambridge, CB3 0ET, UK
[b] Department of Earth Science and Engineering, Imperial College London, London, SW7 2AZ, UK
[c] Department of Geology and Geological Engineering, Colorado School of Mines, Golden, CO 80401, USA
[d] Lawrence Livermore National Laboratory, P.O. Box 808, Livermore, CA 94551, USA
[e] Berkeley Geochronology Center, Berkeley, CA 94709, USA
[f] School of Earth and Climate Sciences and the Climate Change Institute, University of Maine, Orono, ME 04469, USA
[g] Department of Geography and Environmental Sciences, Northumbria University, Newcastle-upon-Tyne, NE1 8ST, UK

ARTICLE INFO

Handling editor: C. O'Cofaigh

Keywords:
Quaternary
Glaciology
Antarctica
Glacial geomorphology
Glaciation
Holocene
Erratic
Glacial geology
Ice doline
Pine Island Glacier

ABSTRACT

The Hudson Mountains are situated in the eastern Amundsen Sea sector of the West Antarctic Ice Sheet, adjacent to Pine Island Glacier. They form a volcanic field of 17 stratovolcanoes and parasitic vents, preserved as nunataks. Two former tributaries of Pine Island Glacier (Larter and Lucchitta glaciers) flow through the mountains. Here we present a detailed study of the glacial geology of the area. We describe field observations and measurements of geomorphological features from 15 of the nunataks, meltwater ponds found on the surface of three nunataks and supraglacial features (ice dolines) from two sites near the present grounding line. Together these provide constraints on the past ice sheet extent, flow pathways and thermal regime, and enhance our understanding of the present hydrological regime – all of which are important as context for the observed modern ice sheet behaviour.

We find evidence suggesting that all nunataks in the Hudson Mountains were covered by ice during the Last Glacial Maximum (defined here as 26.5-19 ka; Clark et al., 2009) and have since deglaciated. Faceted and polished erratic cobbles and boulders of exotic lithologies (syenites, alkali granites, granites, granodiorites, tonalites and gabbros) are numerous and perched on nunatak surfaces. A marked difference between the dominant erratic lithologies on nunataks adjacent to Pine Island Glacier (granite) and Lucchitta Glacier (granodiorite-tonalite) indicates that the ice sheet was transporting clasts from at least two distinct upstream source regions. The similarity in degree of weathering suggests, however, that all the erratics were transported by one phase of (warm-based) glaciation; their presence on or close to the summits of all except one nunatak indicates that the ice sheet during that time was at least 700 m thicker than present. These results are consistent with ice sheet model simulations which suggest that all nunataks in the Hudson Mountains were completely submerged by the Last Glacial Maximum ice sheet.

1. Introduction

This paper describes the glacial geology of the Hudson Mountains, a series of 17 remote and rarely visited volcanic nunataks situated in the eastern Amundsen Sea sector, adjacent to Pine Island Glacier (PIG; Fig. 1a). The Amundsen Sea sector of the West Antarctic Ice Sheet contains several major ice streams (Thwaites, Pine Island, Pope, Smith, and Kohler glaciers) that are dominating the present-day contribution from Antarctica to sea level rise (Rignot et al., 2019; Smith et al., 2020). These ice streams are grounded on retrograde beds that slope inland towards the centre of the ice sheet and are largely below sea level (Morlighem et al., 2020), characteristics which together make them particularly vulnerable to dynamic instabilities that have the potential to cause rapid ice mass loss (Weertman, 1974; Thomas and Bentley, 1978). As a result, the Amundsen Sea sector has attracted a high level of attention from researchers in the past decade, especially those focusing

* Corresponding author.
E-mail address: jsj@bas.ac.uk (J.S. Johnson).

https://doi.org/10.1016/j.quascirev.2024.109027
Received 22 July 2024; Received in revised form 23 October 2024; Accepted 23 October 2024
Available online 3 January 2025

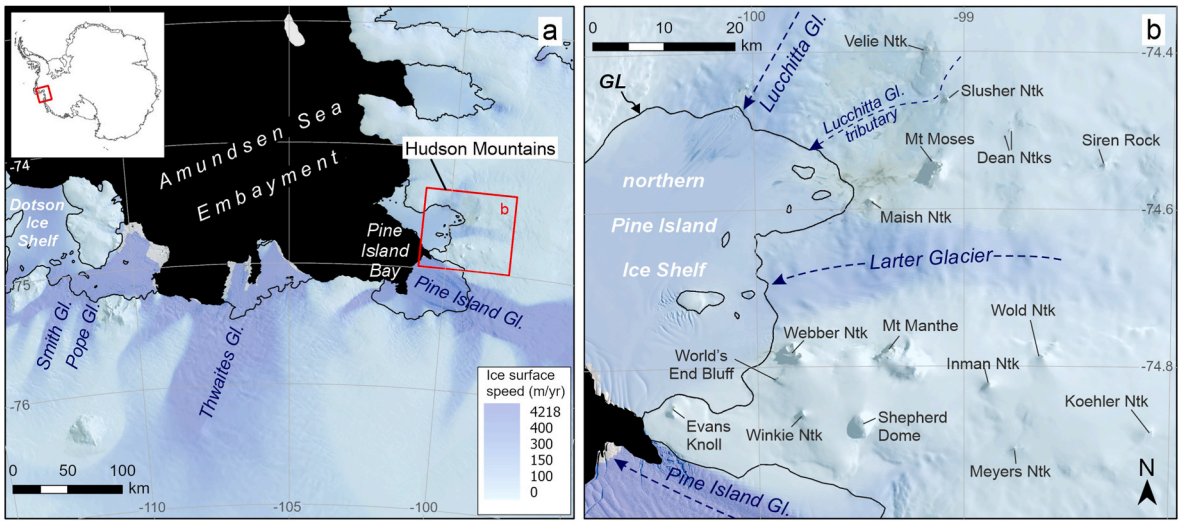

Fig. 1. Study area. (a) Location of Hudson Mountains in relation to wider Amundsen Sea Embayment. (b) Locations of Hudson Mountains nunataks relative to Pine Island, Larter and Lucchitta glaciers. The grounding line (2011; solid black line, labelled '*GL*' in panel b) is from Rignot et al. (2016) and Gerrish et al. (2024) and the coastline is from SCAR Antarctic Digital Database [Accessed: July 2024]. Ice surface speeds (Rignot et al., 2017) are overlain on Landsat Image Mosaic of Antarctica (LIMA; Bindschadler et al., 2008) in panel (a) and a Landsat-8 Image acquired on March 13, 2022, courtesy of the U.S. Geological Survey, in panel (b).

on ice sheet dynamics and the role of the ocean in driving ongoing retreat (Scambos et al., 2017). However, studies of its glacial history have been relatively sparse. This is largely because the rock outcrops in the Amundsen Sea sector are extremely remote and seldom visited. Thus, despite considerable interest in the region and the recognised importance of palaeo records for providing context for the observed contemporary ice sheet behaviour, no detailed report of its glacial geology or geomorphology has yet been published.

The Hudson Mountains rise to 874 m asl and consist of both basaltic lavas and associated clastic rocks that are thought to have erupted 4.9–32.8 Ma ago (Rowley et al., 1986). The upper sequences of two of the peaks are presently covered by an ice dome (the higher of which rises to 960 m asl), whereas the other summits are all exposed. The southernmost peaks are adjacent to the main trunk of PIG. Larter Glacier and Lucchitta Glacier, formerly tributaries of PIG when the grounding line extended beyond Evans Knoll (Fig. 1b; see Johnson et al., 2014), flow through the central and northern Hudson Mountains, respectively. The flow of both glaciers is currently restrained by the northern Pine Island Ice Shelf (Fig. 1b). Recent retreat of the grounding line of PIG has resulted in its calving front retreating close to the promontory on which Evans Knoll is situated (Arndt et al., 2018; Joughin et al., 2021), effectively detaching the northern Pine Island Ice Shelf.

The Hudson Mountains were first visited in 1968 by a joint US-USSR-Chilean geological field party (Wade and Craddock, 1969), but then not again for nearly 50 years until, in 2006, researchers supported by the German research vessel RV *Polarstern* used helicopters to access two of the nunataks for geological studies (Johnson et al., 2008; Werner et al., 2007). Since then, there have been further visits by British, German and Russian field parties in 2007, 2010, 2019-20 and 2022-23, although the Russian campaigns in 2007 and 2010 were biological surveys only (Lupachev and Abakumov, 2013) and the 2022-23 campaign focused on subglacial drilling (Johnson et al., 2024). Here we present glacial geomorphological observations and measurements made primarily during the 2019-20 field campaign and discuss the implications of our findings for understanding of past ice sheet configuration and behaviour in this important region.

2. Methods

A survey of the geomorphological features, glacial deposits and glacio-lacustrine features in the Hudson Mountains was undertaken in the 2019-20 austral summer season, from three field camps established near Webber Nunatak, Wold Nunatak, and Mount Moses (Fig. 1b). All but two of the peaks (Velie Nunatak and Koehler Nunatak) in the Hudson Mountains were visited. The survey was undertaken during a field campaign whose primary purpose was to survey the bedrock geology and glaciology at grounding line-proximal sites as candidate locations for a forthcoming subglacial bedrock drilling campaign (Johnson et al., 2024); thus, time available at each nunatak for glacial-geological survey was limited and not all parts of each nunatak were visited. Topographic maps compiled using Sentinel-2 satellite imagery by the British Antarctic Survey Mapping and Geographic Information Unit were used for geolocation, planning travel routes, and for recording field observations. The survey involved looking for evidence of former ice cover such as the presence on bedrock surfaces of glacial striations, erratic cobbles/boulders of exotic lithology, and glacial till.

We collected samples from erratic cobbles and boulders from all 15 of the visited nunataks with the purpose of supplementing previous sampling campaigns (for surface exposure dating) that focused on selected nunataks only (see Johnson et al., 2008, 2014). Exposure ages from 41 erratics from the Hudson Mountains, including some of those collected in 2019-20, are already published and provide evidence for rapid deglaciation of PIG in the mid-Holocene (Johnson et al., 2008, 2014; Nichols et al., 2023). The remaining samples are part of an ongoing study (that will include further exposure age dating not presented here) to determine the deglacial history of Larter and Lucchitta glaciers. The locations of all these samples are shown on maps in Figs. S10–S25 (Supplementary Data). We measured the position (latitude, longitude, elevation) of each feature or deposit with a Javad Triumph II GPS receiver and corrected the heights above ellipsoid to orthometric heights (height above geoid EGM08). Prior to sampling, we photographed the erratics, and made measurements of their size, morphology (shape and roundness), long axis orientation and weathering characteristics. We derived the erratic shapes from measurements of the lengths of long, intermediate and short axes of each erratic, with the long axis length used to classify its size as a small cobble (0–20 cm), medium cobble (20–35 cm), large cobble (35–50 cm), boulder (50–100 cm) or large boulder (>100 cm). The degree of roundness of each erratic was determined by a visual assessment and comparison with the Powers roundness scale (Powers, 1953). Orientations of the longest axis of the erratics were measured as magnetic bearings and corrected to true bearings (reported in this paper) using the magnetic declination of 46°E.

Table 1
Weathering classification used in the present study.

Weathering classification
W_1: Heavily weathered surface, surrounded by spallation products; no iron staining or pitting on upper surface
W_2: Moderately weathered surface, iron stained, with some spalling/pitting of upper surface
W_3: Intact slightly weathered surface, unspalled
W_4: Fresh surface, unweathered, unspalled

All data are provided in Table S1. We also recorded the orientation of striations visible on bedrock surfaces (Table S2). The degree of weathering of erratics was assessed by visual comparison, using a weathering index simplified from existing schemes published by Owen et al. (2009), Moriwaki et al. (1994) and White et al. (2009) (Table 1). After sampling, we classified the lithology of each cobble using visual estimation of the modal proportions of constituent minerals plotted on a QAPF diagram (Streickheisen, 1976).

Geomorphological data were collected only for cobbles (90 in total) that were sampled for exposure dating. The dataset presented here therefore does not provide a comprehensive evaluation of all erratics present in the Hudson Mountains because it includes only a subset of them. When sampling for exposure dating, we prioritised collection of exotic erratics perched on horizontal or gently sloping bare/scoured bedrock (i.e. entirely free of till, sediment, soil or snow) to minimise the chance of periodic snow cover or post-depositional movement associated with periglacial activity or mass wasting. Of these, we preferentially collected cobble-sized erratics with the following characteristics: (i) quartz-bearing lithology, or if none were present, olivine-bearing lithology, (ii) evidence of glacial shaping/erosion such as polish, striated surfaces, and smooth rounded to sub-angular shape (rather than angular), and (iii) minimal weathering or surface pitting/spalling. Our sampling was not biased towards greater sphericity or degree of polish/striation. Although our adherence to these criteria implies that our dataset could be biased towards smaller rounded erratics and those whose lithology is suitable for cosmogenic nuclide measurement, the majority we observed (not just those we sampled) in the Hudson Mountains are cobble-sized, relatively rounded and do contain quartz or olivine. Thus, we think the subset we measured is representative of at least the size range, degree of roundness and lithological diversity of all erratics in the area.

Here we use the recorded erratic morphology data (shape and roundness) to investigate the history of glacial transport (following Benn and Ballantyne, 1993). In addition to the measurements and observations from our 2019-20 field campaign, we include data from two further groups of samples: (i) the size, shape, orientation and lithology of erratics from two of the Hudson Mountains nunataks, Mount Moses and Maish Nunatak (Fig. 1b), collected during 2010 (on RV *Polarstern* cruise ANT-XXVI/3, by JAS) and (ii) the size, shape and lithology of two erratics from Mount Manthe (Fig. 1b) sampled in 2006 (by JSJ). All of the samples are listed under the Hudson Mountains in "ICE-D: Antarctica", an informal cosmogenic nuclide exposure age database for Antarctica (https://www.ice-d.org/antarctica/[accessed June 25, 2024]; Balco, 2020). We classified the lithologies by visual assessment of the constituent minerals, as for the 2019-20 erratics. Since morphological information was not routinely recorded in either of the earlier surveys, we estimated the approximate size and long axis orientation of the 2010 erratics and assessed their roundness using a combination of field photographs and measurements made in the laboratory prior to preparing the erratics for cosmogenic nuclide analysis. For the Mount Manthe erratics sampled in 2006, we determined the size and degree of roundness from field photographs and notes but were unable to reconstruct the long axis orientations.

In order to explore patterns in the morphological and orientation data, we analysed those data using several methods, as follows. The shape data, derived from measurements of the lengths of the long, intermediate and short axes of each cobble, were plotted on ternary diagrams (cf. Sneed and Folk, 1958; Benn and Ballantyne, 1993) using TriPlot, an Excel spreadsheet designed specifically for this purpose (Graham and Midgley, 2000). We calculated the C40 index (percentage of clasts with short to long axis ratios $\leq$0.4) to provide a further indication of erratic shape (cf. Benn and Ballantyne, 1993, 1994). We plotted histograms of the resulting roundness data to determine the relative degrees of roundness of erratic cobbles at each site. Finally, we calculated the Relatively Angularity (RA) index (percentage of angular and very angular clasts in a sample) to determine whether there is any correlation of angularity with transport distance (Benn and Ballantyne, 1994).

3. Results

Here we describe the glacial features and deposits, supraglacial lakes and other meltwater-related features observed in the Hudson Mountains. We divide our descriptions of evidence for past glaciation into three groups, reflecting the glacier or tributary that most likely deposited the glacial erratics observed on each nunatak (Fig. 2 and Table 2).

3.1. Glacial features and deposits

3.1.1. Nunataks adjacent to Pine Island Glacier (Group I)

The six peaks of this group – Evans Knoll, Winkie Nunatak, Shepherd Dome, Inman Nunatak, Meyers Nunatak and Koehler Nunatak – are situated 6–25 km from the northern margin of PIG in the southern Hudson Mountains (Fig. 1b). They form a transect from Evans Knoll, close to the grounding line, to Koehler Nunatak furthest (~75 km) upstream. The highest peak (Koehler Nunatak) rises to 874 m asl at its summit, approximately 524 m above the adjacent surface of PIG (Table S3). The lowest, Evans Knoll (summit 254 m asl), is situated adjacent to the northern Pine Island Ice Shelf (Fig. 1b). Shepherd Dome (750 m asl) is a largely ice-covered dome with bedrock outcropping only on its southern side, whereas the other peaks in this group all have a proportionally much greater area of exposure. We did not visit Koehler Nunatak; however, field notes from the party that visited the site in 1968 record that there are "many irratics [*sic*] of granite" present on the (basaltic scoria) bedrock there (Schaefer, initial unknown, 1968). This observation suggests a similar past glacial cover to other nunataks in the Hudson Mountains.

The bedrock at all the Group I nunataks is volcanic, consisting predominantly of pillow lavas with less common volcaniclastic sequences, the latter of which are intruded by mafic dykes at Evans Knoll, Inman and Meyers nunataks. No patterned ground was observed at any of the sites, but frost shattering (e.g. Fig. 3a) is very common. Evans Knoll is the only site in Group I where we observed bedrock striations: the surface of a mafic dyke (near sample EVK-101) is strongly striated in a NNE-SSW direction (Table S2; Fig. S10).

We observed erratic cobbles, and rarely boulders, scattered across the bedrock surfaces up to the summits of all five nunataks we visited (their presence at Koehler Nunatak, in addition, is confirmed by Schaefer, initial unknown, 1968). The erratics we sampled range from 11 to 89 cm diameter (predominantly small cobbles with long axis <20 cm; Fig. 4a) and are commonly rounded to sub-rounded (e.g. Fig. 3b), with very low RA and C40 indices (both $\ll$40; Fig. 4b) that together indicate subglacial – rather than supraglacial – transport (Benn and Ballantyne, 1994; Lukas et al., 2013). On a ternary diagram, the erratics largely fall in the central zone, indicating no overall preferred shape (Fig. S7a; cf. Lukas et al., 2013 fig. 1). Several very large (>1 m-sized; Fig. 3b and c) erratic boulders were observed (but not sampled) at Evans Knoll but are absent on the other nunataks adjacent to PIG. Erratics are relatively scarce at Inman and Meyers nunataks compared with the nunataks further downstream. For example, the upper slopes of Evans Knoll — the site nearest the modern grounding line — are covered with

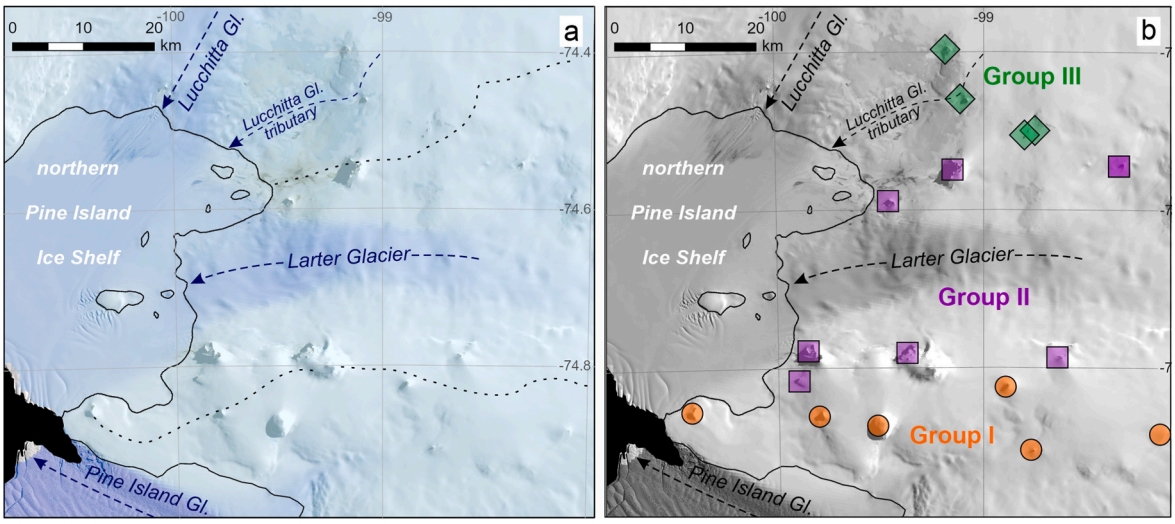

Fig. 2. Ice divides and associated groups of Hudson Mountains nunataks (see text). (a) Map showing location of main ice divides (dotted lines). (b) Map showing locations of nunataks in each group. Group I: orange circles; Group II: purple squares; Group III: green diamonds. Imagery and data sources as the same as for Fig. 1a. For clarity, the ice surface speed is shown in greyscale in panel (b).

extensive deposits of glacial till in which abundant cobbles are embedded or perched (Fig. 3c), whereas Inman and Meyers nunataks (and to a lesser extent Shepherd Dome) host many fewer, and more sparsely distributed, erratics of generally smaller size (typically small cobbles of <20 cm diameter; Fig. 3d, 3e, 3f and 4a). Small amounts of residual till are, however, present in gulleys on the northern side of Inman Nunatak. The till blanketing the upper slopes of Evans Knoll (between ~200 m asl and the summit at 254 m asl) consists predominantly of granitic clasts of 2–15 cm size embedded within a finer matrix (Fig. 3c). Some of these granitic clasts are very degraded, presumably as a result of post-depositional weathering or frost shattering. Also present in the till are a few clasts of the same lithology as the basaltic bedrock that is exposed on the lower slopes of the nunatak. At Inman Nunatak, the till contains a higher proportion of angular clasts and more diverse lithologies, reflecting the range of erratic cobbles perched on bedrock there (Fig. 3f and Fig. S2). Moraines were not observed at any nunataks in Group I.

The erratics at all sites adjacent to PIG are composed predominantly of granite and alkali granite (Fig. 4c, Figs. S1 and S2), but other exotic lithologies such as greyish-green volcanic cobbles, gabbros and syenites were observed at Inman (Fig. 3f and Fig. S2), Winkie and Meyers nunataks (Figs. S1 and S2). The alkali granite and syenite erratics frequently contain abundant orthoclase feldspar, giving them a strong salmon-pink colour in hand specimen. The predominant degree of weathering of the erratics we observed is slight to moderate (weathering index W_2-W_3), with a few unweathered cobbles (index W_4) present on Meyers Nunatak and Shepherd Dome. The most weathered cobbles/boulders have a slight brown patina. Evidence of glacial transport, such as faceting and polish of the erratics, are common at Evans Knoll and Winkie Nunatak, where the surfaces of many are also striated (Fig. 3a). The preferred orientation direction of the long axes of the erratics sampled at this group of nunataks is WNW-ESE (Fig. 4b), which aligns with the present-day flow direction of Pine Island Glacier (Fig. 1) but is orthogonal to the orientation of bedrock striations at Evans Knoll (NNE-SSW; Table S2).

3.1.2. *Nunataks adjacent to Larter Glacier (Group II)*

The seven peaks in this group are located adjacent to Larter Glacier which flows into the northern Pine Island Ice Shelf (Fig. 2b). Those outcropping on the glacier's northern side are Maish Nunatak, Mount Moses and Siren Rock, and those on its southern side are Webber Nunatak, World's End Bluff, Mount Manthe, and Wold Nunatak. They form a transect from Webber and Maish nunataks, very close to the grounding line, to Wold Nunatak and Siren Rock approximately 40 km upstream. The highest point in the Hudson Mountains is Mount Manthe, whose ice dome rises 470 m above an exposed cliff section to reach 960 m asl at the summit (Table 2). The highest subaerially-exposed peak in the Hudson Mountains, Siren Rock, rises to 835 m asl at its summit, closely followed by Mount Moses at 833 m asl. Although the summits of both are of almost equal elevation, the ice-free area on Mount Moses is much greater, with bedrock outcropping continuously on its western side from 220 m asl.

The bedrock of the nunataks in this group consists of basaltic lavas and volcaniclastic sequences. World's End Bluff is unique in the Hudson Mountains in that its bedrock (tuff) contains pink cobble-sized clasts (approximately 5 % in total) which appear from binocular observations to be granitic in composition. We were unable to sample or measure these clasts due to their exposure only in an inaccessible steep cliff section that descends on the western side of the outcrop towards the northern Pine Island Ice Shelf. However, several cobbles with similar lithology and size to these clasts are strewn across the accessible upper surface of the outcrop raising the possibility that the cobbles weathered out of the underlying bedrock, rather than being deposited on its surface during glaciation. Due to this uncertainty, we do not include cobbles from World's End Bluff in our study.

We did not observe patterned ground at any of the sites, but frost shattering is common, particularly where there are lavas outcropping at the surface, such as at Maish and Webber nunataks and Mount Manthe. Evidence of past ice cover is present on the lower slopes of Mount Moses (at ~460 m asl) in the form of strongly striated and truncated pillow lava (bedrock) surfaces (Fig. 5a). The striations are oriented ~ N-S (Table S2 and Fig. S20). None were observed at higher elevations on Mount Moses. We also observed striated bedrock in small (<10 cm^2) patches at Webber Nunatak (Table S2), with orientations ~ N-S, ~NW-SE and NW-SE (Fig. S17) and at Mount Manthe where striations oriented ~ N-S extend over several metres (Fig. S18). All striations at Group II nunataks are of millimetre-scale, closely spaced and near-parallel, consistent with erosion by warm-based ice.

Erratic cobbles and boulders are scattered across the bedrock surfaces of most nunataks in this group, including up to the summits of Mount Moses and Siren Rock. The erratics studied range from 10 to 150 cm diameter (but are predominantly small and medium cobbles with long axis <35 cm; Fig. 4d) and are predominantly sub-angular (Fig. 4e). Several very large (>1 m-sized) erratic boulders were observed, and occasionally sampled, at all sites in this group except Mount Manthe and

Table 2
Glaciers flowing through the Hudson Mountains, and related nunataks. Asterisks indicate peaks that were not visited by the authors and are thus not included in the present study.

Group	Glacier/tributary	Related nunataks	Latitude (DD)	Longitude (DD)	Summit elevation (m asl)
I	Pine Island Glacier	Evans Knoll	−74.85	−100.41	254
	Pine Island Glacier	Winkie Nunatak	−74.86	−99.78	500
	Pine Island Glacier	Shepherd Dome	−74.88	−99.54	n.d. *(750)*[c]
	Pine Island Glacier	Inman Nunatak	−74.82	−98.87	792
	Pine Island Glacier	Meyers Nunatak	−74.91	−98.75	630
	Pine Island Glacier	Koehler Nunatak*	−74.88	−98.08	n.d. *(874)*
II	Larter Glacier	Webber Nunatak	−74.77	−99.83	579
	Larter Glacier	World's End Bluff[a]	−74.81	−99.91	242
	Larter Glacier	Mount Manthe	−74.78	−99.40	n.d. *(960)*[c]
	Larter Glacier	Maish Nunatak	−74.59	−99.46	n.d., but >286[b] *(269)*
	Larter Glacier	Mount Moses	−74.55	−99.14	833
	Larter Glacier	Wold Nunatak	−74.79	−98.63	760
	Larter Glacier tributary	Siren Rock	−74.54	−98.33	835
III	Lucchitta Glacier tributary	Slusher Nunatak	−74.46	−99.08	617
	Lucchitta Glacier tributary	Velie Nunatak*	−74.40	−99.18	n.d. *(621)*
	Lucchitta Glacier tributary	Dean Nunatak crater	−74.50	−98.78	696
	Lucchitta Glacier tributary	Dean Nunatak knoll	−74.51	−98.80	626

[a] Denotes a site which was visited but whose cobbles have an ambiguous depositional history and cannot therefore be confidently attributed to glaciation (see section 3.1.2).
[b] Summit height based on highest erratic collected. Elevations of all other summits were measured using a Javad Triumph II GPS receiver (see methods). n.d. = not determined; summit heights acquired from the Reference Elevation Model of Antarctica (REMA; Howat et al., 2019) for those sites are provided in italics.
[c] Height of ice dome covering upper sequences (see Fig. 10 for visual representations).

Siren Rock (Fig. 4d). There is a higher proportion of angular and very angular erratics present in this group (RA index: 10) than in Group I (RA index: 3). Nevertheless, as for Group I, both the RA and C40 indices are low (≪40; Fig. 4e), indicating subglacial transport. On a ternary diagram, Group II erratics fall largely in the central zone, indicating no overall preferred shape (Fig. S7b). Ventifacted erratics in the Hudson Mountains (e.g. Fig. 5b and sample MTM-03, Fig. S3) are uniquely associated with Mount Moses. Ventifacts were observed on the lower slopes of the NW face of the nunatak and a col just below the summit, both adjacent to extensive deposits of volcanic ash which were likely responsible for their formation via abrasion by wind-transported ash particles.

The abundance of erratics varies considerably between different sites in this group. In contrast to the abundance of cobbles and boulders at Maish and Wold nunataks (Fig. 5c and d), erratics are present at Webber Nunatak, Mount Manthe, Mount Moses and Siren Rock, but are scarce and restricted to small areas on each outcrop. At Mount Manthe they occur only on the top of a platform (at ~480 m asl; Johnson et al., 2008) formed by sub-horizontal basalt lava sequences (cf. fig. C.9.2., Rowley et al., 1986), presumably because the underlying volcaniclastic flows form steep-sided cliff faces that cannot support cobbles or boulders. At Siren Rock, erratics occur almost entirely only on the side closest to Larter Glacier (see Fig. S22), but despite their scarcity (e.g. Fig. 5e), they are present within 5 m of the summit. In contrast, erratics are conspicuously absent above 237 m asl at Webber Nunatak (342 m below the summit, 70 m above the modern ice margin) and are present only in small numbers on the lower sections of two ridges on the Larter Glacier side of the nunatak (Fig. 6a and Fig. S17). Striated bedrock surfaces (see above) are the only evidence for past ice cover anywhere else on the nunatak despite its summit at 579 m asl (Table 2) being significantly lower in elevation than other Group II sites where erratics are abundant, for example Wold Nunatak. Although Mount Moses has the largest ice-free area of all the Hudson Mountains peaks, erratics there are similarly scarce and are confined to the southern and western faces and the summit ridge (Fig. S20). The highest erratic observed at Mount Moses is at 800 m asl (MOS-104), just below the summit.

The erratics at the sites adjacent to Larter Glacier are composed of granite, alkali granite, granodiorite and tonalite, with some having a foliation fabric such as gneissic banding while others display igneous layering or porphyritic textures (Figs. S3–S5). There is a visible difference in the lithologies present on these nunataks compared with those in Group I adjacent to PIG (Figs. S1 and S2). Erratics at the Group I sites are dominated by pink alkali granites and granites (whose pink colour originates from the abundance of orthoclase feldspar and is also noticeable in the syenites). In contrast, at Group II sites, fewer granitoids contain orthoclase feldspar (resulting in more that are pale grey/white in colour). At Mount Moses, the vast majority of erratics we observed are pale grey granite, granodiorite or tonalite (Figs. S3 and S4). However, in contrast, erratics at sites nearest to the grounding line in the same group – Maish Nunatak, Webber Nunatak and Mount Manthe – are predominantly composed of the same orthoclase-rich alkali granite lithology that is typical of Group I sites. Thus, the erratic populations at Group II sites appear to become poorer in alkali granites and richer in tonalites with distance from the grounding line, with the highest proportion of tonalites observed at Siren Rock (Fig. S4) and rare erratics of basaltic or other volcanic composition occurring only at Wold Nunatak (Fig. 5f; note: these rarer erratics are not captured in Fig. 4f because they were not sampled). Fabrics or distinct textures are common in the Group II and III erratics (those of granodiorite and tonalite lithologies in particular), but absent in Group I.

As for Group I, the predominant degree of weathering at nunataks in Group II is slight to moderate (weathering index W_2-W_3), with a few unweathered cobbles (W_4) observed at Wold Nunatak and Siren Rock. The most weathered erratics have pitted surfaces. Faceting and polishing of the (pink alkali granite) erratics was observed at Maish (Fig. S3), Webber and Wold (Fig. S5) nunataks. Erratics from Group II nunataks are oriented in multiple directions, with preference towards WNW-ESE orientations, and to a slightly lesser extent NE-SW (Fig. 4e). These align with the present-day flow direction of Pine Island Glacier and Lucchitta Glacier, respectively (Fig. 1b).

Moraines occur close to the ice margin at two Group II sites, Mount Moses and Webber Nunatak (none were observed elsewhere in the Hudson Mountains). At the SW foot of Mount Moses, binocular observation identified two dark-coloured rocky exposures (approximately 250 × 45 m and 50 × 60 m) surrounded by ridges of ice. We were unable to determine whether the underlying surface is composed of rock or ice. The moraine's location is at the point where ice flowing around the north and south sides of Mount Moses converges, thus it is a likely site for deposition of glacially transported material and development of a moraine. An extensive moraine at the western end of Webber Nunatak (Fig. 6a) close to the modern grounding line likewise occurs at the confluence of ice flowing around the eastern and western sides of the

Fig. 3. Field photographs of glacial deposits on the surfaces of nunataks adjacent to Pine Island Glacier. (a) Cobble with striated surface perched on frost shattered bedrock at Winkie Nunatak. (b) Rounded boulder at Evans Knoll. (c) Glacial till covering the upper slopes of Evans Knoll. (d) Relatively sparse distribution of erratics at Meyers Nunatak; a lone cobble can be seen perched on the rubbly bedrock in the foreground. (e) Two perched erratic cobbles on the summit of Inman Nunatak. (f) Erratic cobbles of varying exotic lithologies at Inman Nunatak.

nunatak. The moraine is ice-cored, with a thin layer of locally derived basaltic lava rubble mixed with abundant granitoid cobbles draped on the surface, forming hummocks several metres in height (Fig. 6b). The cobbles are a variety of sizes (some >50 cm diameter) and include prominent pink granite and grey granodiorite gneisses. Since the moraine is ice-cored, it must have formed sometime between the Last Glacial Maximum (LGM, defined here as 26.5-19 ka; Clark et al., 2009) and present, probably in an ice-marginal setting.

There is a distinctly visible difference in the dominant lithology of the erratics on the northern and southern sides of the moraine. Granodiorite erratics dominate on the northern side, whereas pink granite erratics dominate on its southern side. The granite erratics become gradually scarcer towards the glacier on the southern side of Webber Nunatak and are entirely absent from the moraine on its most southerly outcrop, implying that ice flowing around the southern side of Webber Nunatak did not transport much englacial material (Fig. 6b). This observation corroborates our interpretation of cobbles at World's End Bluff being weathered out of the bedrock, rather than deposited by ice.

3.1.3. Nunataks adjacent to the tributary of Lucchitta Glacier (Group III)

This group consists of four outcrops in the northern Hudson Mountains – Velie Nunatak, Slusher Nunatak and two with the official name 'Dean Nunataks'. Velie Nunatak is situated 27 km from the grounding line on the northern margin of a tributary of Lucchitta Glacier which

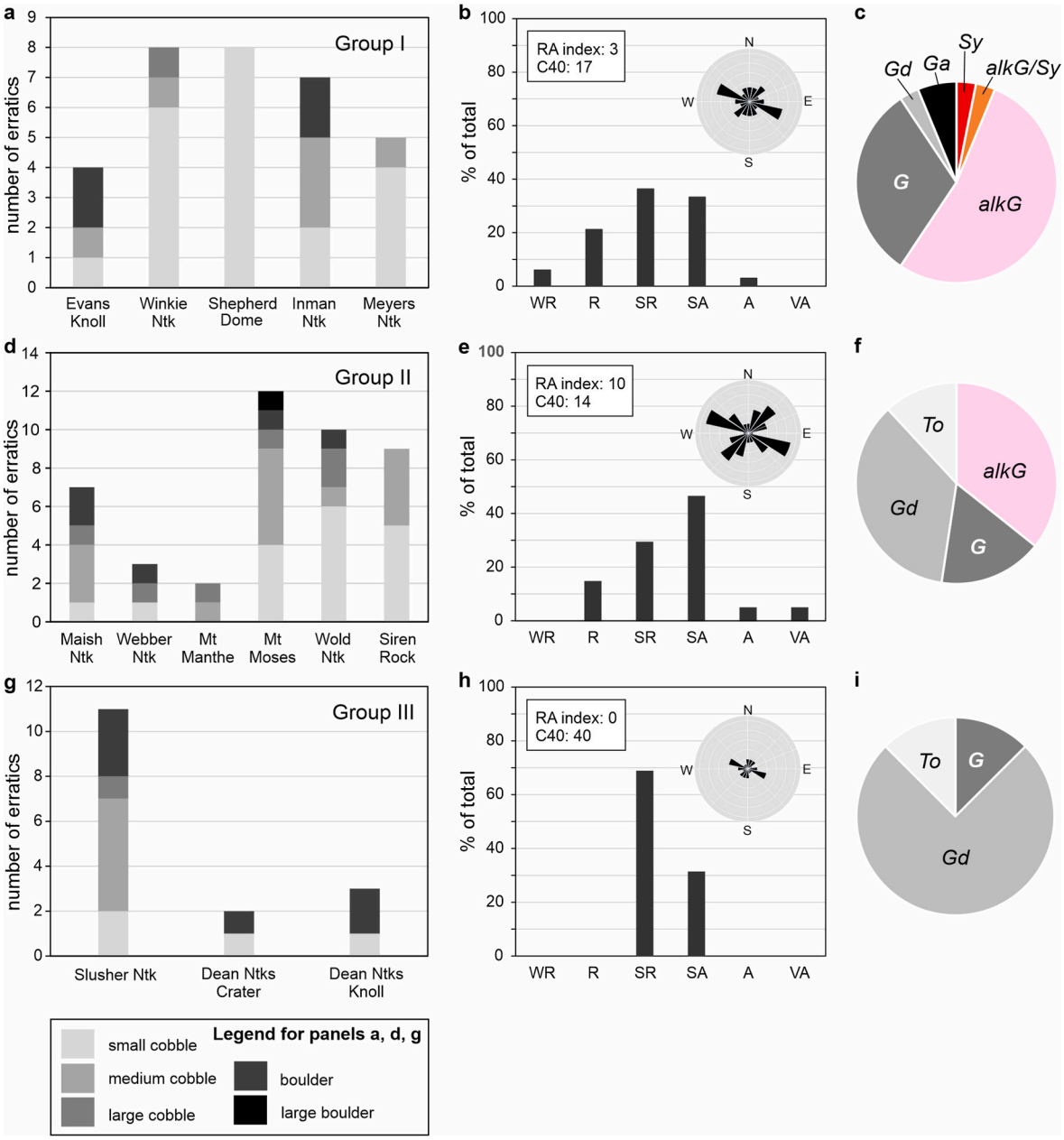

Fig. 4. The shape, orientation and lithology of erratic cobbles sampled in the Hudson Mountains. **Top row** (panels a–c): sites adjacent to PIG - Group I; middle row (panels d–f): sites adjacent to Larter Glacier - Group II; bottom row (panels g–i): sites adjacent to Lucchitta Glacier - Group III. **First column** (panels a, d and g): histograms showing size of erratics. For PIG, Larter and Lucchitta glaciers respectively, n = 32, 43 and 16. **Second column** (panels b, e and h): Histograms showing degree of cobble roundness (WR = well-rounded, R = rounded, SR = sub-rounded, SA = sub-angular, A = angular, VA = very angular) and orientation, each with an inset rose diagram showing long axis orientations. Note the orientations of the cobbles are plotted on the rose diagrams in both directions, so the total number of cobbles shown is twice the number actually measured. Five of the 32 cobbles in Group I, seven of the 43 in Group II and one of the 16 in Group III are equant and are therefore not included in the respective rose diagrams. The RA and C40 indices are also shown (see text). **Third column** (panels c, f and i): Pie charts showing proportions of erratic lithologies represented in each nunatak group. Lithologies classified according to the QAPF classification of Streickheisen (1976): To = tonalite, G = granite, Gd = granodiorite, alkG = alkali granite, Sy = syenite, Ga = gabbro.

feeds the northern Pine Island Ice Shelf (Fig. 1b). The nunatak was not visited by the authors, and field notes from the last known visit to the site in 1968 (Schaefer, initial unknown, 1968) make no mention of any evidence for past ice cover, even though the presence of erratics and/or striated surfaces are occasionally mentioned for the other nunataks the party visited. The glacial geology of Velie Nunatak therefore remains unknown. Slusher Nunatak is situated approximately 20 km from the grounding line adjacent to the same tributary, and Dean Nunataks are situated 8 km upstream of Slusher Nunatak. In the field, we informally named (and hereafter call) the two outcrops of Dean Nunataks 'Dean Nunataks Knoll' and 'Dean Nunataks Crater'. They consist of a small (300 × 200 m) exposed area of basalt bedrock (Dean Nunataks Knoll) that rises only 10 m above the modern ice sheet surface, and a circular crater-like outcrop of 450 m diameter (Dean Nunataks Crater; Fig. 7a) situated 1 km to the NE. Dean Nunataks Crater rises to 696 m asl, 80 m above the local ice sheet surface. Slusher Nunatak is slightly lower, with an elevation of 617 m asl at its summit, and a total relief of 92 m. Dean Nunataks Crater is unique in the Hudson Mountains both in its shape and its bedrock characteristics. In contrast to the only other circular feature found in the area, a dome with three small (~40 × 20 m) outcrops of

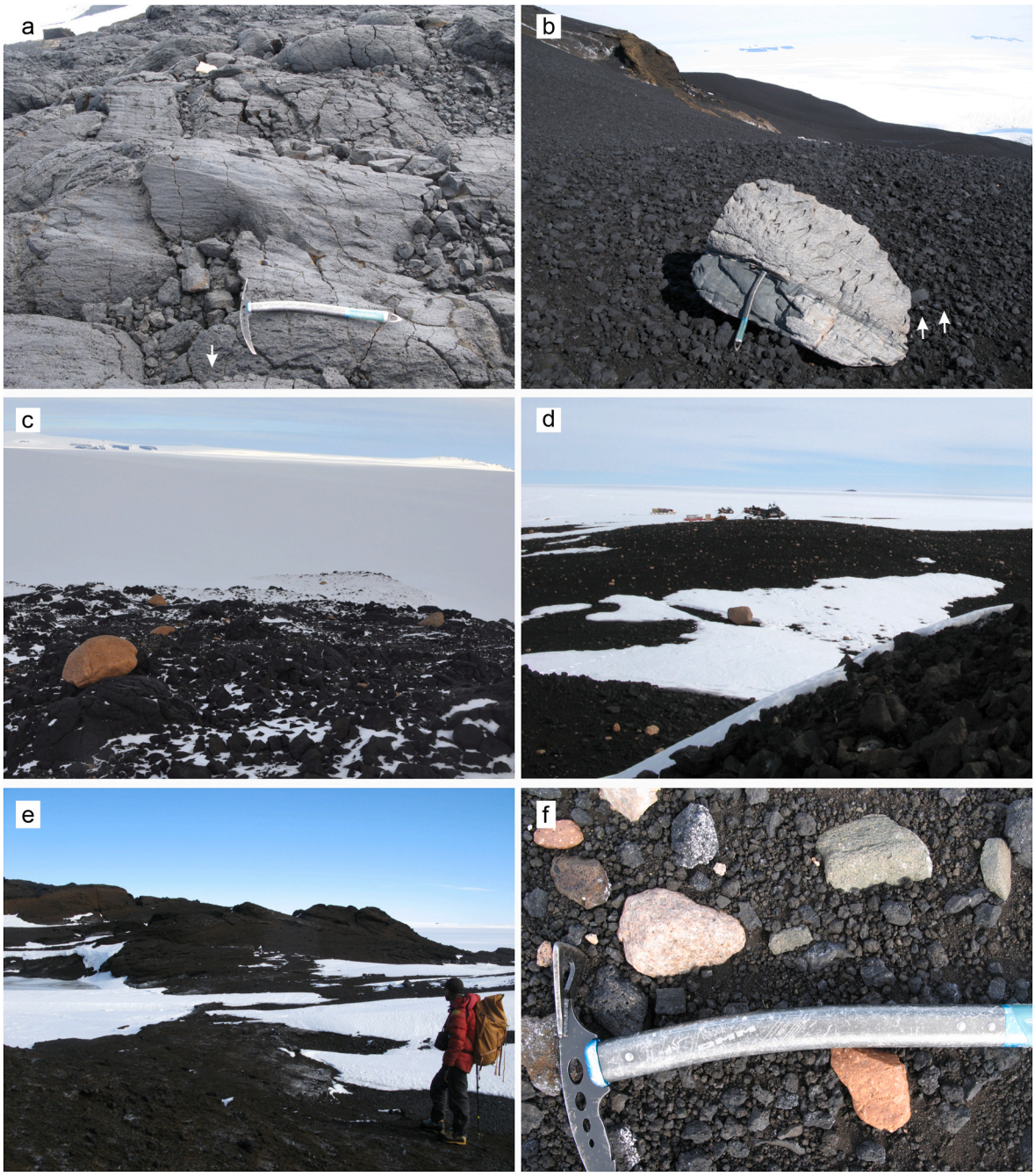

Fig. 5. Field photographs showing evidence of past glaciation and/or post-depositional erosion on the surfaces of nunataks adjacent to Larter Glacier and its tributary. (a) Striated bedrock pillow lavas at Mount Moses. (b) Ventifacted erratic boulder at Mount Moses. (c) Abundant large pink alkali granite erratics strewn on the basaltic lava bedrock at Maish Nunatak. (d) Abundant granitoid erratics perched on lava at Wold Nunatak. (e) The SW side of Siren Rock showing absence of any erratics, which, if present, would be clearly visible against the dark coloured basaltic bedrock. (f) Exotic erratics at Wold Nunatak, including rare greenish volcanic clasts of a lithology that does not crop out locally or elsewhere in the Amundsen Sea sector.

rock on top (Shepherd Dome, Group I), it has the form of an exposed annular rim surrounding an ice-filled central depression (Fig. 7a). Unlike any of the other Hudson Mountains, it is composed almost entirely of reddened basaltic scoria (Fig. 7b).

Evidence for past ice cover, in the form of cobbles and boulders of exotic lithology, is ubiquitous at both Dean Nunataks outcrops and Slusher Nunatak. No other evidence for past glaciation, such as striated bedrock or glacial landforms, was observed. Furthermore, there is no till at any of the sites and the bedrock at Slusher Nunatak is intact, not extensively frost shattered as at Dean Nunataks Crater and Knoll. Patterned ground is visible at both Dean Nunataks Crater and Knoll (but not at Slusher Nunatak). Erratics are widely distributed at Dean Nunataks Knoll but are scarcer than at many other sites in the Hudson Mountains. At Dean Nunataks Crater, the erratics similarly occur up to the summit (Fig. 7a) but are even less common than at Dean Nunataks Knoll. At both sites, erratics of a wide range of sizes occur, including some large erratic boulders with diameter >50 cm (Fig. 7c) as well as several smaller cobbles <30 cm diameter. They are all of similar lithology to the erratics found at Mount Moses and Siren Rock in Group II (predominantly granodiorite and tonalite; Fig. 7b, Figs. S3 and S4). In contrast to Dean Nunataks Knoll and Crater where erratics are sparse, abundant erratic cobbles and boulders are widely-distributed over

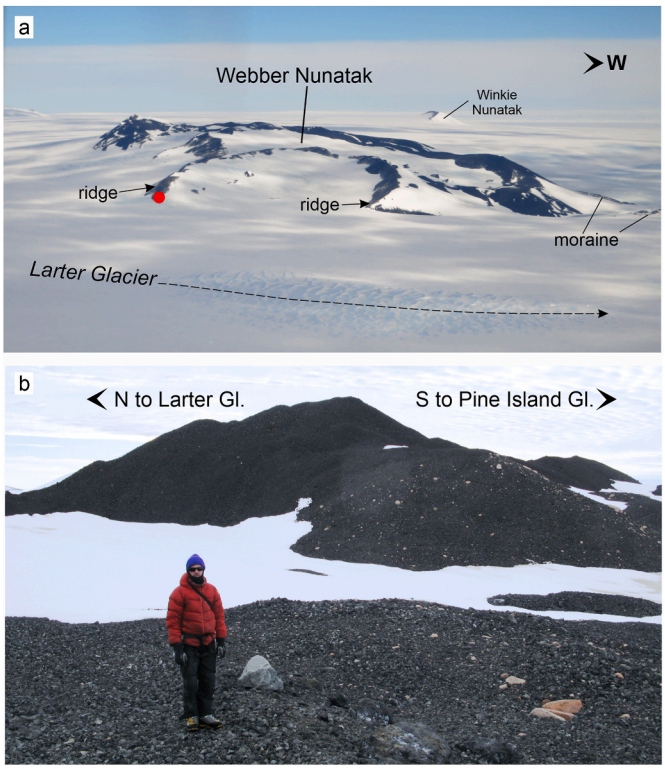

Fig. 6. Webber Nunatak. (a) Photograph overview of nunatak looking to the south, showing location of two ridges extending towards Larter Glacier and a moraine at its western end. Erratics are present only at the base of the ridges and were collected for this study only from the location indicated by the red circle. (b) Close-up view of moraine at western end of Webber Nunatak, looking east (upstream). Pale grey granodiorite erratics are visible towards the northern side of the moraine (left of image), whilst pink granitic erratics are dominant toward the southern side of the moraine (right of image). The abundance of the granitic erratics decreases towards the south. Person for scale.

Slusher Nunatak (Fig. 7d). Many of them are faceted and polished (Fig. 7e), and dominantly sub-rounded and elongated in shape, consistent with englacial transport. The site has the most abundant erratics of all sites in the Hudson Mountains, akin to Evans Knoll but more varied in lithology and perched on bare bedrock, rather than till or frost shattered lavas. Erratics were found on the summit of Slusher Nunatak as well as on its lower slopes. Some of the granodioritic erratics contain the mineral garnet, which was not observed elsewhere in the Hudson Mountains, either in erratics or exposed bedrock.

The erratics we sampled from Group III nunataks range from 11 to 69 cm diameter (predominantly small and medium cobbles with long axis <35 cm; Fig. 4g) and are all sub-rounded or sub-angular (Fig. 4h; RA index: 0). Their preferred long axis orientation is WNW-ESE (Fig. 4h), which aligns with the present flow direction of PIG (Fig. 1). Based on our observations across all sites in the Hudson Mountains, the size range of the erratics at Slusher Nunatak is greater than at many other sites (Fig. 4g): as well as cobbles, we observed many boulders with >50 cm diameter, and some as large as 2 m diameter (Fig. 7c), the largest seen by us anywhere in the area (note, none of the very large >1 m-sized erratic boulders at Slusher Nunatak were sampled). In contrast to the very low C40 indices for erratics in Groups I and II, Group III erratics have a higher – although still low overall – C40 index (40; Fig. 4h). This suggests a greater abundance of elongated erratics (e.g. Fig. 7e) in this group, consistent with more abrasion occurring during glacial transport. Whilst this difference in shape is not corroborated by their position on a ternary diagram where they plot in the central zone overlapping with those in Groups I and II (Fig. S7), evidence of abrasion such as faceting and glacial polish were commonly observed in the field (see above). The dominant degree of weathering of all the erratics we sampled from sites in Group III is consistent with those of Groups I and II: slight to moderate (weathering index W_2-W_3), with a handful of unweathered cobbles (index W_4; observed at Slusher Nunatak).

3.2. Supraglacial lakes and other meltwater-related features

During the 2019-20 season, we observed pools of liquid water on several of the Hudson Mountains nunataks, and also on the ice sheet nearby. Whilst these do not provide evidence of past glacial activity, they provide information about the presence and accumulation of meltwater, which can impact local glacial dynamics. We found supraglacial meltwater ponds several metres in diameter very close to the modern grounding line near Webber and Maish nunataks. On the ice shelf adjacent to Maish Nunatak, there are two water-filled ice dolines, with circular rings of liquid water surrounding a frozen centre (Fig. 8a). On the ice shelf adjacent to Webber Nunatak, a similar outer ring of liquid water surrounding a frozen core is visible adjacent to the moraine at the western end of the nunatak (Fig. 8b). The uplifted rim, centre and inverted forebulge (i.e. surface 'moat') occupied by water are characteristic of dolines that periodically drain into ice shelves. The meltwater accumulation is either a result of surface melting, snow melt from the adjacent nunataks, or a combination of both. The appearance of the dolines at Webber and Maish nunataks is similar to that of lakes situated over ice shelves elsewhere on the Antarctic Ice Sheet (e.g. Amery Ice Shelf; Warner et al., 2021; George VI Ice Shelf; Banwell et al., 2024).

In addition, we found ponds containing liquid water in depressions in the bedrock at Mount Moses and Slusher Nunatak, and two ponds that were frozen – although we visited one in March when temperatures are typically lower than December/January – at Mount Manthe (details given in Table 3, with photographs in Fig. 9 and Fig. S8). At Mount Moses, the two higher ponds we observed are linked by a narrow stream. In contrast, the pond at Slusher Nunatak appears to be isolated. It is supplied with snowbank melt with seepage areas sloping towards the pond (Fig. 9d), rather than being fed by meltwater flowing from nearby glaciers. Both ponds observed at Mount Manthe (Fig. 9c and Fig. S8a) are situated immediately in front of glacial ice (in an 'ice marginal' setting), indicating that they are formed by surface meltwater creating a flat ice surface between the glacier and the bedrock. At all the ponds, we found lines and patches of salt efflorescence on many of the surrounding bedrock surfaces, sometimes extending up to 2 m above the present water level (e.g. at Mount Moses; Fig. 9a). This salt efflorescence is presumably related to past periods of higher water levels (cf. Hodgson and Bentley, 2013) or the presence of snow patches that have repeatedly melted and evaporated. Although salt efflorescence is present, we did not see any other geomorphological evidence (e.g. raised beaches) for former shorelines at any of these locations. The presence of liquid water demonstrates that the bedrock dominating the area (yellowish brown lapilli tuffs and dark grey basalt lavas) can absorb enough solar radiation, and thereby emit sufficient heat, to cause localised melting of snow and ice. We did not determine the salinity of the water within the ponds, but it is likely that the closed-basin pond (Table 3) has accumulated salts that would contribute to a lower freezing point.

4. Discussion

The observations and measurements described above provide information about the extent of past glaciation in the Hudson Mountains, including thickness, flow direction and basal regime of the PIG system. We discuss our interpretations of each of these elements below, as well as the present-day glacial dynamic context obtained from our observations of meltwater ponds and ice dolines.

4.1. Present environmental conditions

Several ponds and water-filled ice dolines, both in the ice sheet and

Fig. 7. Field photographs of glacial deposits on the surfaces of northern nunataks adjacent to the Lucchitta Glacier tributary. (a) Panoramic view of Dean Nunataks Crater looking northwards (skidoos circled, for scale). Erratics, indicated by arrows, are rare at this site. (b) Pale coloured granodiorite erratic, with size 18 x 14 x 8 cm, perched on reddened (oxidised) scoriaceous lava at Dean Nunataks Crater. (c) Very large erratic boulder perched on bedrock at Slusher Nunatak (person for scale). (d) Abundant granitoid erratics perched on bare tuffaceous bedrock at Slusher Nunatak (e) Elongated granodiorite erratic cobble at Slusher Nunatak (rock saw for scale). The cobble is faceted and polished on its uppermost side, indicated by the pinkish colouration.

in depressions in the bedrock surfaces, were identified in the Hudson Mountains during our visit in 2019-20. All of these are visible in Copernicus Sentinel-2 imagery every year (to 2024) since its launch in 2015 — as are several others that we did not visit or observe during fieldwork — implying that they are a recurring feature, persisting at least during the austral summer months. The presence of liquid water in ponds on several of the nunatak surfaces implies that the low albedo of the basaltic lavas that are extensive in the Hudson Mountains (frequently cropping out over several tens to hundreds of metres continuous extent) creates sufficient radiative heat to seasonally melt ice and snow patches to form ponds. In the case of the pond at Slusher Nunatak, if it is closed to surface outflow as we suspect, the resulting elevated salinity may also contribute to the presence of liquid water (cf. Hodgson et al., 2010). Salt efflorescence observed on the surrounding bedrock surfaces above the ponds (Fig. 9a) may imply that water levels have been higher in the past (at least 2 m higher at Mount Moses, although we were not able to determine when this occurred). The lack of palaeo-shorelines at any of the ponds we visited suggests that these periods of higher water level are likely to have been short-lived. Several supraglacial lakes close to the present grounding line of Larter Glacier, particularly around Mount Moses, Maish and Webber nunataks (Fig. 1b), provide evidence of seasonal surface melting or meltwater from the adjacent nunataks. Some are water-filled ice dolines, formed during periods when englacial water has drained into the underlying ice sheet/shelf, resulting in characteristic doline expression at the surface (Fig. 8). Their presence implies a dynamic hydrological regime at the grounding line of Larter Glacier and periodic delivery of meltwater to its bed, consistent with a warm-based (erosive) thermal regime at the base of the ice sheet (Brisbourne et al., 2017).

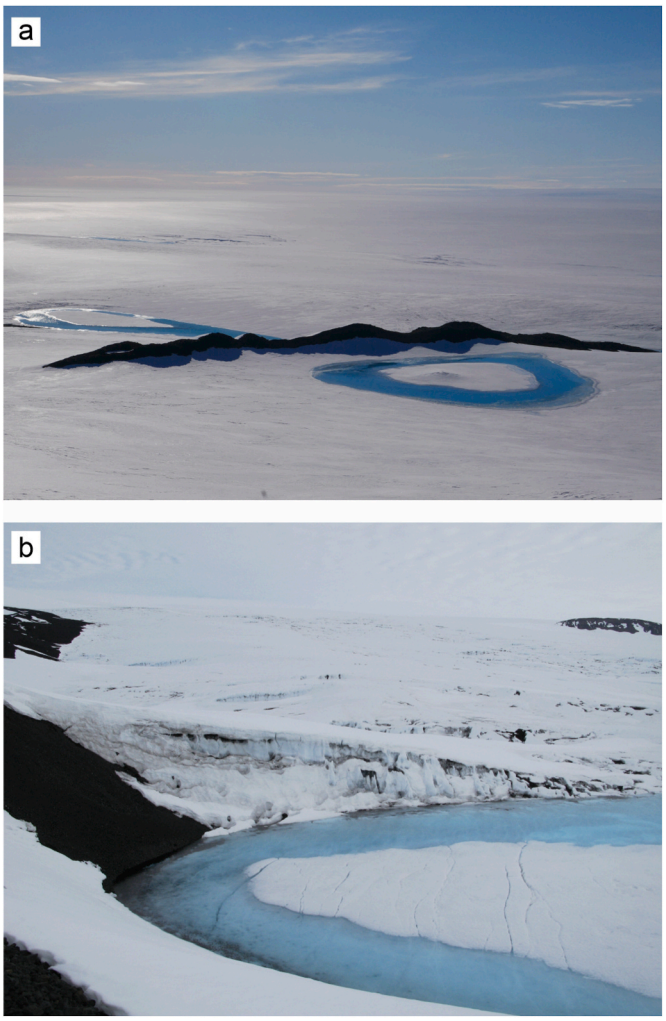

Fig. 8. Water-filled ice dolines next to (a) Maish Nunatak (at −74.59516 S/−99.45578 W and −74.59607 S/−99.47941 W) and (b) Webber Nunatak (at −74.78342 S/−99.91205 W). In each case, a circular ring of liquid meltwater surrounds a frozen centre.

4.2. Extent of past glaciation

Almost all nunataks in the Hudson Mountains have cobbles and boulders of non-local lithology perched on their surfaces up to (or to within a few metres of) their summits. Many of those cobbles and boulders have polished and/or faceted surfaces, and our analysis of their dimensions and shapes produced low C40 and RA indices that together suggest they were transported subglacially (cf. Lukas et al., 2013). We therefore interpret them as being glacially transported and then left stranded on the nunatak surfaces as the grounding line of PIG retreated and the glacier and its tributaries subsequently thinned. To have deposited an erratic, the ice sheet must have been at least as thick as the present elevation of that erratic; the elevation ranges of the erratics (Fig. 10) can thus be used to determine minimum past ice sheet thickness. The highest exposed summit that we visited in the Hudson Mountains is 835 m asl (Siren Rock; Fig. 1b), which is 323 m above the present elevation of the centreline of Larter Glacier (512 m asl; Fig. 10b), and 728 m above PIG (107 m asl; Nichols et al., 2023). Since erratics occur close to that summit, we conclude that the ice sheet surface must have been at or above 835 m asl at some time in the past. The reputed presence of granitic erratics lying on bedrock at Koehler Nunatak (Schaefer, initial unknown, 1968) which rises to 874 m asl is further evidence that the ice sheet surface was above 800 m asl in the past. The highest point in the area is the ice dome of Mount Manthe (960 m asl; Fig. 10b), which rises above a flat-topped sequence of lavas. It is highly likely that the upper sections of this peak have been ice-covered since the LGM, implying that the ice sheet surface was even higher (closer to 1000 m asl) than indicated by the erratics at Koehler Nunatak.

Since most of the erratics we observed are only slightly weathered or fresh, it is likely that they were all deposited in the Hudson Mountains during the last glacial period and became ice-free only since then. This suggestion is corroborated by surface exposure ages from sites adjacent to PIG and Larter Glacier (including most of the nunataks in Group I, and Maish Nunatak, Mount Moses and Mount Manthe in Group II), which indicate that those sites were ice-covered at the LGM and became ice-free around 8 ka (Johnson et al., 2008, 2014; Nichols et al., 2023). K-Ar dating of volcanic sequences at Mount Manthe and Velie Nunatak yielded eruption ages of 3–8 Ma (Rowley et al., 1986), suggesting that it is unlikely that any of the nunataks in the Hudson Mountains postdate the last glaciation. An LGM ice sheet at least 700–800 m thicker than present matches model simulations of the last retreat of Pine Island Glacier that imply that all of the Hudson Mountains nunataks would have been ice-covered at that time (cf. fig. 8, Johnson et al., 2021). Furthermore, and consistent with complete submergence of the nunataks during the last glacial period, we did not observe any trimlines that would provide evidence for a maximum ice level (Sugden et al., 2005).

Webber Nunatak is the only peak in the Hudson Mountains to have erratic cobbles and (rarely) striations present *only* on its lowermost surfaces (<324 m asl; 247 m above modern ice), raising the possibility that its summit and higher elevations remained ice-free when other summits in the area were glaciated. As one of the closest Hudson Mountains peaks to the present grounding line (Fig. 10), the location of Webber Nunatak means it should be sensitive to past changes in ice sheet elevation. Given that we found evidence for past ice-cover at all nunataks upstream (where most summits are higher; Table 2), as well as at others proximal to the grounding line (e.g. Evans Knoll and Maish Nunatak), it seems highly likely that Webber Nunatak's summit was also ice-covered despite the apparent lack of geomorphological evidence. It is common for pillow lavas – which dominate at Webber Nunatak – not to preserve signs of erosion by ice. This appears to be the case elsewhere in the Hudson Mountains (e.g. on the summit of Mount Moses where erratics indicating former ice-cover are present but where the surrounding bedrock is not striated; see section 3.1.2). Our observations at Webber Nunatak, including the preservation of delicate glassy vesicular rims on pillow lavas, are consistent with the presence of cold-based

Table 3
Location and size/depth estimates of ponds observed in the Hudson Mountains. Depth estimates are given only where the pond is liquid throughout, or only partially frozen, and where the bottom could be clearly seen. All sites were visited in December 2019 or early January 2020, except for the Mount Manthe site marked with an asterisk, which was visited in March 2006 (by JSJ).

Location	Type	Figure	Latitude (DD)	Longitude (DD)	Elevation (m asl)	Estimated size (m)	Estimated depth (m)
Mount Moses	in bedrock depression/open	S8b	−74.54757	−99.17186	456	12 x 5	1
Mount Moses	in bedrock depression/open	9a	−74.54134	−99.16942	469	30 x 15	0.5
Mount Moses	in bedrock depression/open	9b	−74.54997	−99.17102	470	30 x 20	1
Mount Manthe	ice marginal/open	9c	−74.78976	−99.41260	490	100 x 50	n.d. (frozen)
Mount Manthe*	ice marginal/open	S8a	−74.77633	−99.36082	485	370 x 200	n.d. (frozen)
Slusher Nunatak	in bedrock depression/?closed	9d	−74.46043	−99.08831	559	10 x 5	1 (partially frozen)

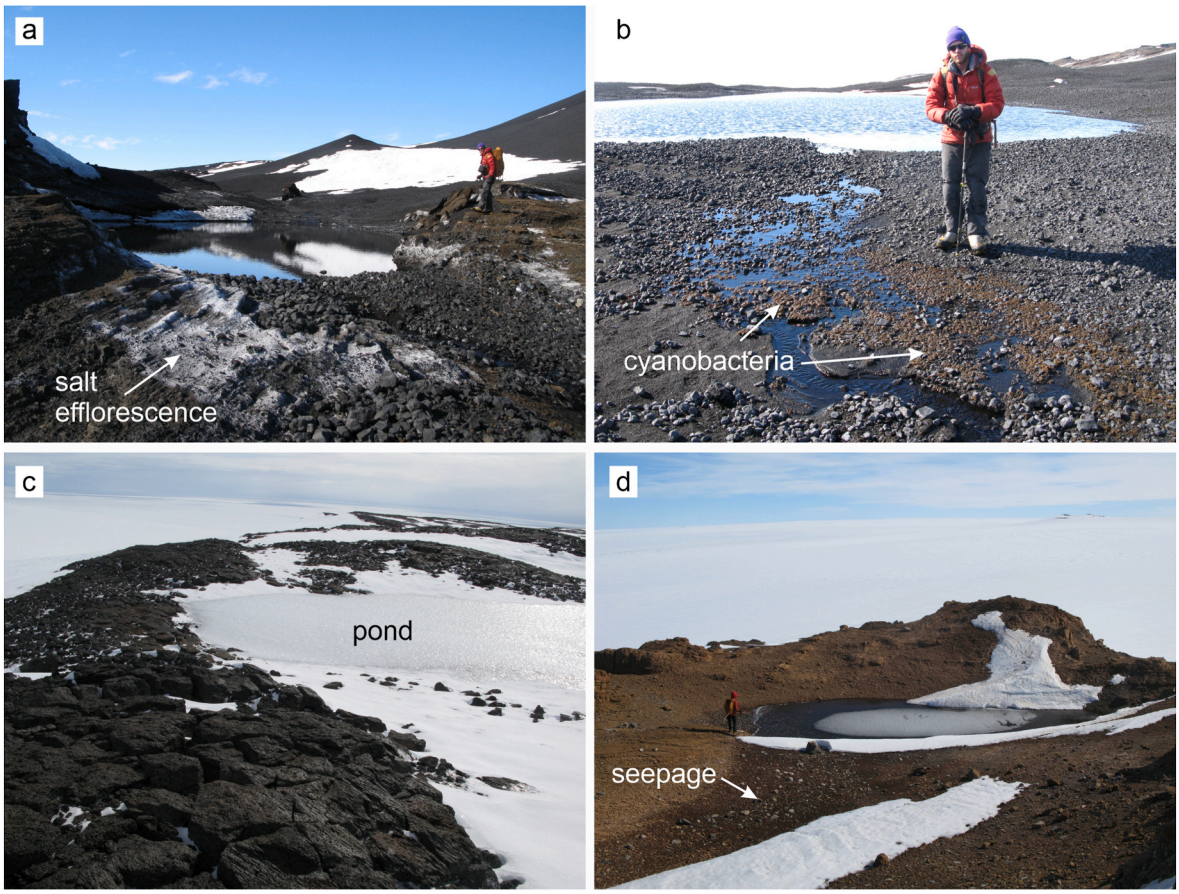

Fig. 9. Ponds in the Hudson Mountains. Location details are given in Table 3. (a) Pond (with reflections) at Mount Moses. White efflorescence on rocks in foreground is salt encrustation that may indicate previously higher water levels. (b) Pond in a second shallower bedrock depression at Mount Moses, fed by a stream seen in foreground. The brownish growth adjacent to the stream consists of cyanobacterial mats. (c) Pond in bedrock depression at Mount Manthe; frozen during our visit in December 2019. (d) Partially frozen pond at Slusher Nunatak. The darkish patch towards the bottom of the photograph indicates seepage into the pond. Cyanobacteria were found at the pond edge where liquid water is present.

(non-erosive) ice covering the summit of Webber Nunatak while ice flowing between the nunatak and the peaks surrounding it was warm-based, erosive and transporting erratics from upstream. This situation could have resulted in Larter Glacier preferentially depositing erratics on the margins of Webber Nunatak (and also forming the moraine at its western end; Fig. 6) rather than on its higher sections. The striations on the lower sections of Webber Nunatak are consistent with such a hypothesis; they are oriented radially outward towards Larter Glacier (Fig. S17), indicating past ice flow directed away from the summit rather than parallel to Larter Glacier. We note that an ice dome presently covers the upper elevations of Mount Manthe while a few erratics were observed on an exposed area below (Fig. 10b); Mount Manthe may therefore provide an analogy for how Webber Nunatak may have looked prior to deglaciation of its summit ice cover. A similar interpretation of cold-based ice cover was made at Mount McClung in Marie Byrd Land where, in contrast to all surrounding peaks, erratics are absent (Sugden et al., 2005). Holocene in situ ^{14}C exposure ages on Mount McClung's bedrock (unpublished, but available under site 'MCG' in the ICE-D: Antarctica database; https://www.ice-d.org/antarctica/) indicate that the summit of Mount McClung was nevertheless deglaciated at the same time as the surrounding peaks. Our hypothesis that the summit of Webber Nunatak was ice-covered during the LGM and deglaciated in the Holocene could in future be confirmed by surface exposure dating using in situ ^{14}C extracted from olivine present in the basaltic bedrock (Johnson et al., 2024).

4.3. Environment of past transport and deposition

The size, shape and lithological diversity of erratics can provide information on the properties of the ice that transported them and potentially also on the relative distances they have travelled. The relatively high degree of rounding in the Hudson Mountains cobbles indicates that they probably originated in a zone of warm-based ice upstream and were subject to extensive erosion during glacial transport. Although a few boulders of >1 m diameter are present at Evans Knoll, Mount Moses, and Inman and Slusher nunataks, the vastly greater prevalence of small and medium cobbles across the Hudson Mountains region is added evidence for transport within a highly erosive environment; such transport would reduce the size of larger boulders and cobbles through abrasion, favouring deposition of an array of smaller clasts. An erosive setting is further corroborated by surface exposure age data obtained from nunataks in Groups I and II. Erosion during glacial transport removes the inherited ^{10}Be nuclide inventory in both erratics and bedrock, but if erosion is not sufficient, some ^{10}Be will be retained (e.g. Stone et al., 2003; Nichols et al., 2023). The 41 Hudson Mountains erratics analysed thus far all yielded ^{10}Be exposure ages in the range 5.1–14.0 ka, with only three older than 8.3 ka, demonstrating the apparent absence of significant ^{10}Be inheritance from exposure prior to the last glacial period (Johnson et al., 2008, 2014; Nichols et al., 2023).

Although the size and shape of all the Hudson Mountains erratics are broadly similar, there are some differences between the three tributary groups. These are discussed in detail in the Supplementary Data (Appendix A). We interpret the differences as evidence for a strong

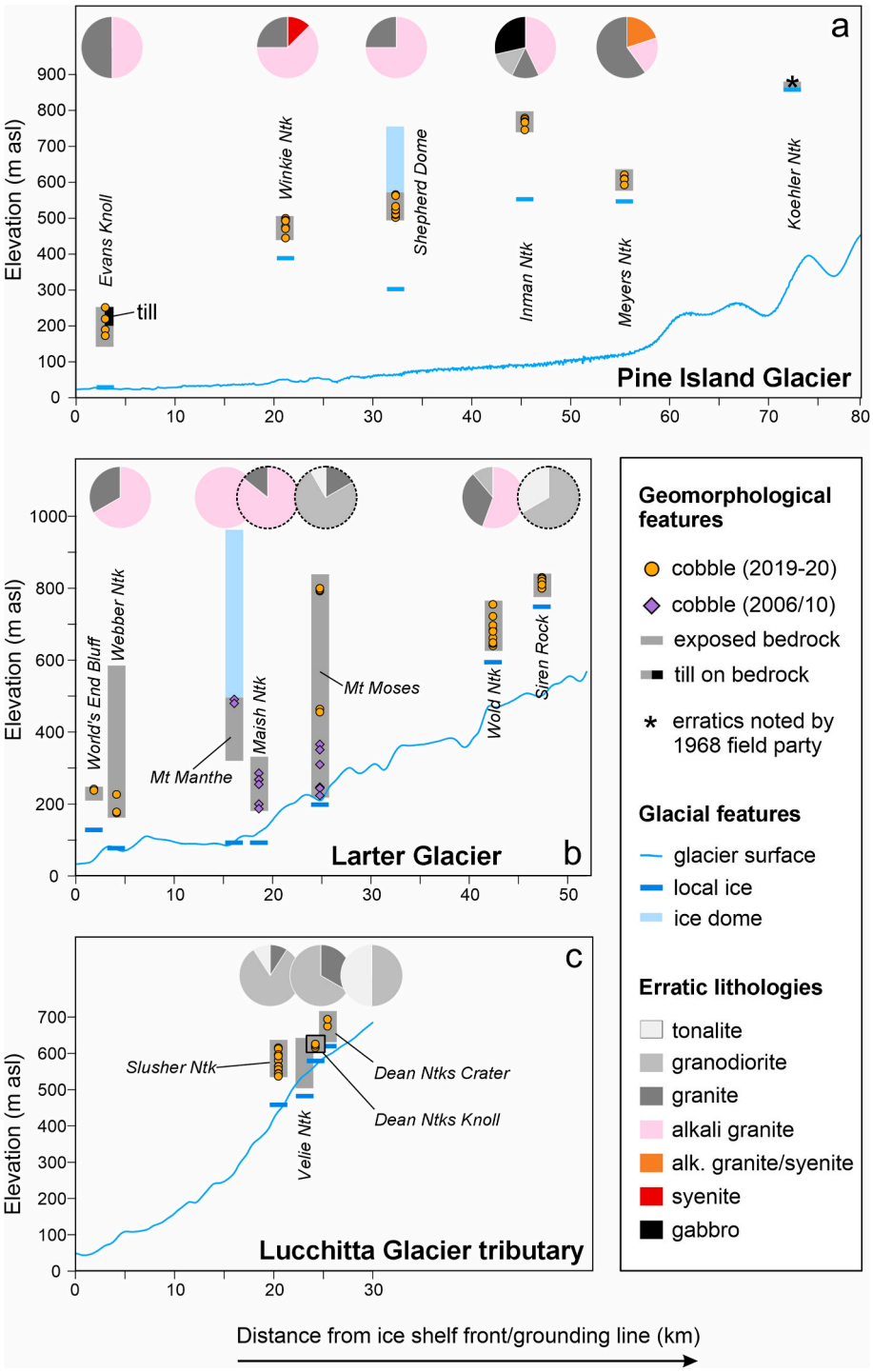

Fig. 10. Profiles along flowlines of glaciers in the Hudson Mountains, showing altitude and lithologies of erratics used in this study, location of till deposits, and elevation range of exposed rock/ice domes. (a) Profile along PIG. Since all but one of the nunataks are now downstream of the 2011 grounding line when projected onto the centreline of the glacier, the x-axis here represents distance from the ice shelf front. (b) Profile extending 50 km along Larter Glacier from the 2011 grounding line. Pie charts with dashed outlines represent erratic lithologies on nunataks situated on the northern side of Larter Glacier; those without outlines are those on the southern side. (c) Profile extending 30 km along Lucchitta Glacier tributary from the 2011 grounding line. The blue line in each panel represents the present ice sheet surface profile and is taken from REMA (Howat et al., 2019). The 2011 grounding line is from Rignot et al. (2016) and Gerrish et al. (2024). The pie charts show the proportions of different erratic lithologies represented in the samples we collected from each site.

lithological influence on erratic morphology. This is demonstrated firstly by the existence of a higher proportion of sub-angular clasts in Group II (indicated by RA index) which are also dominantly granodiorite and tonalite lithologies. To test whether angularity is influenced by lithology, we calculated RA indices using only the granitic erratics. The result is almost no difference in the proportions of angular clasts between the three nunatak groups. Secondly, the degree of platiness of clasts (indicated by C40 index) is greater in Group III erratics than in the other groups. When only granites are included in the analysis, C40 is lower for all groups, but substantially lower for Group III erratics suggesting that erratics of non-granitic lithologies tend to be more platy/elongated than their granitic counterparts. Thus, we conclude that clast

shape as well as angularity is strongly controlled by lithology and that we cannot draw any inferences about glacial transport processes or distances from either characteristic.

There are also variations in the lithological diversity of clasts deposited on nunataks in each group (Fig. 10). Of the erratics we measured, the greatest overall diversity of clast lithologies exists in Group I, where only the tonalite lithology appears unrepresented (Fig. 10a). The most diverse of all the nunataks is Inman Nunatak (Group I; Fig. 10a) which hosts erratics of at least four different lithologies; in addition, several other nunataks across all groups (Winkie and Meyers nunataks in Group I, Wold Nunatak and Mount Moses in Group II, Slusher Nunatak in Group III) have at least three different lithologies represented. In contrast, Mount Manthe (Group II) is unique in having erratics of only one lithology (Fig. 10b). Despite these differences, there does not appear to be any systematic variation in diversity of clast lithology with distance from the grounding line. This finding implies that the lithological distribution of erratics is not related to the distance of travel they experienced during glacial transport.

4.4. Pathway of past ice flow and provenance of erratics

The distribution of the erratics provides information on both the pathway of the ice flow that deposited them and their provenance. Erratics are widely distributed across all of the Hudson Mountains, implying that ice flowed across the whole area in the past. The erratic long axis orientations fall broadly into two sets, with preferred orientations of WNW-ESE and NE-SW directions, respectively (Fig. 4). Our sampling strategy minimised the possibility of any post-depositional movement. However, in contrast to clasts that are embedded within till where the till fabric can be used to infer precise flow directions (Evans, 2018), we cannot be certain that the (perched) Hudson Mountains erratics have not moved since emplacement or that they were deposited by lodgement processes under the ice. Thus, using their long axis orientations to infer past flow direction requires caution.

Bedrock striations are a more reliable indicator of former flow direction. Striated bedrock is present, but scarce, in the Hudson Mountains. Furthermore, since the exposure history of bedrock in the area is unknown, it is unclear whether the striations relate to the same glaciation as the erratics. We cannot rule out that the bedrock striations were formed during earlier glaciations — when flow directions may have been different from today — and have been preserved in a few places by the presence of cold-based non-erosive ice. However, the consistently mid-Holocene exposure ages of erratics across the area implies that the nunataks all deglaciated at the same time following the last glacial period. Thus, our observation of two sets of erratic orientations is unlikely to be evidence for two different flow directions during the last glaciation.

The distribution of erratics of different lithologies in the Hudson Mountains can be used to infer the sources of the rocks transported by PIG and its former tributaries. We observed differences in the pattern of distribution of clast lithologies between the southern and northern Hudson Mountains, implying that each glacier transported subglacial bedrock from different upstream source regions. Pink granitic erratics dominate the glacial deposits in the south (closest to PIG), grey granodiorites and tonalites dominate on the northern Larter/Lucchitta Glacier side, and a mixture of these two 'endmembers' exist at nunataks on the southern side of Larter Glacier (Figs. S1–S6; Fig. 10). These findings imply that the PIG source region during and since the last glacial period was dominantly granitic (syenites, alkali granites and granites), whereas the tributary of Lucchitta Glacier was primarily transporting erratics eroded from granodiorite and tonalite bedrock, and Larter Glacier appears to have been transporting a mixture of the two. Furthermore, the greater diversity of clast lithologies observed at sites adjacent to PIG implies that, during and since the LGM, the PIG catchment was probably the largest, transporting material from a wider region than Larter and Lucchitta glaciers, while the catchment of the Lucchitta Glacier tributary was confined to a geographically distinct area sampling a different and more limited array of lithologies. Fig. 11 illustrates a possible ice flow configuration consistent with our observations. Both ice velocities and subglacial bedrock topography (Bedmap-2; Fretwell et al., 2013, not shown) of PIG at the present-day contrast to those of Larter and Lucchitta glaciers and their tributaries, with PIG extending much deeper inland and its upstream tributaries covering over a much wider area. Our interpretation of the lithological distribution of the erratics suggests a similar ice sheet configuration during the last deglaciation.

Since no investigation has yet been undertaken to determine the source of the Hudson Mountains erratics, we are unable to make any detailed inferences about their provenance. However, none of the erratic lithologies we observed crop out within the Hudson Mountains and there are no outcrops along potential ice flow lines between the Hudson Mountains and the southern Antarctic Peninsula/Ellsworth Mountains. Thus, we conclude that the source rocks for all the erratics must lie upstream and below the ice sheet. Palaeozoic—Mesozoic granite and granodiorite basement rocks crop out along the coast of the Amundsen Sea Embayment, at Bear Peninsula (Johnson et al., 2017), Sif Island (Marschalek et al., 2024) and islands in Pine Island Bay (Pankhurst et al., 1998; Mukasa and Dalziel, 2000; Lindow et al., 2014; Kipf et al., 2012; Braddock et al., 2022), but these regions are not glaciologically plausible sources for the erratics because they lie either downstream or outside the current or past flowlines of PIG and its tributaries (cf. Larter et al., 2014). Nevertheless, they provide a snapshot view of rock types that may exist more widely beneath the ice sheet in this region. Geophysical surveys revealed a large subglacial felsic granitoid intrusion immediately south of the main trunk of PIG (Jordan et al., 2023), which suggests there may be other (as yet undiscovered) subglacial granitic bodies in the area that could be the source of some of the erratics.

Our finding that glaciers feeding the area were sampling at least two distinct bedrock source regions during the last glacial period is corroborated by results from provenance of glaciogenic detritus delivered to seafloor sediments – both marine and sub-ice shelf – in Pine Island Bay by PIG and glaciers draining into the northern Pine Island Ice Shelf (Simões Pereira et al., 2020). These results suggest that PIG is underlain by granite and granitoid bedrock of Jurassic and Jurassic-early Palaeozoic age, respectively. In contrast, bedrock upstream of the northern ice shelf consists of Palaeozoic-Mesozoic granitic rocks similar to those outcropping on islands in Pine Island Bay. We therefore surmise that erratics delivered to Group I and III nunataks in the Hudson Mountains probably originate from each of these two source regions, with a mixture from both sources deposited at the Group II sites. Further provenance studies will be required to confirm this hypothesis.

5. Conclusions

Field observations and measurements of glacial geological and geomorphological features collected from 15 nunataks in the Hudson Mountains provide evidence for past ice cover and constraints on the former size and flow dynamics of the Amundsen Sea sector of the West Antarctic Ice Sheet. This information is important for constraining and validating ice sheet models that use geological and geomorphological data. Due to the relative scarcity of glacial landforms in the Hudson Mountains, we have focused our interpretations of glacial history on the glacial deposits. Our main conclusions are:

- Glacial deposits, specifically erratic cobbles of exotic lithology (predominantly granites, granodiorites and tonalites), are present up to the summits of all but one of the 15 nunataks surveyed. The nearly ubiquitous presence of these erratics suggests that all the nunataks were completely submerged by ice at some point in the past and that the ice sheet that deposited them was at least 700 m thicker than present at that time.
- The shape and size of the erratics (predominantly rounded to subangular cobbles of small to medium size) indicates they were

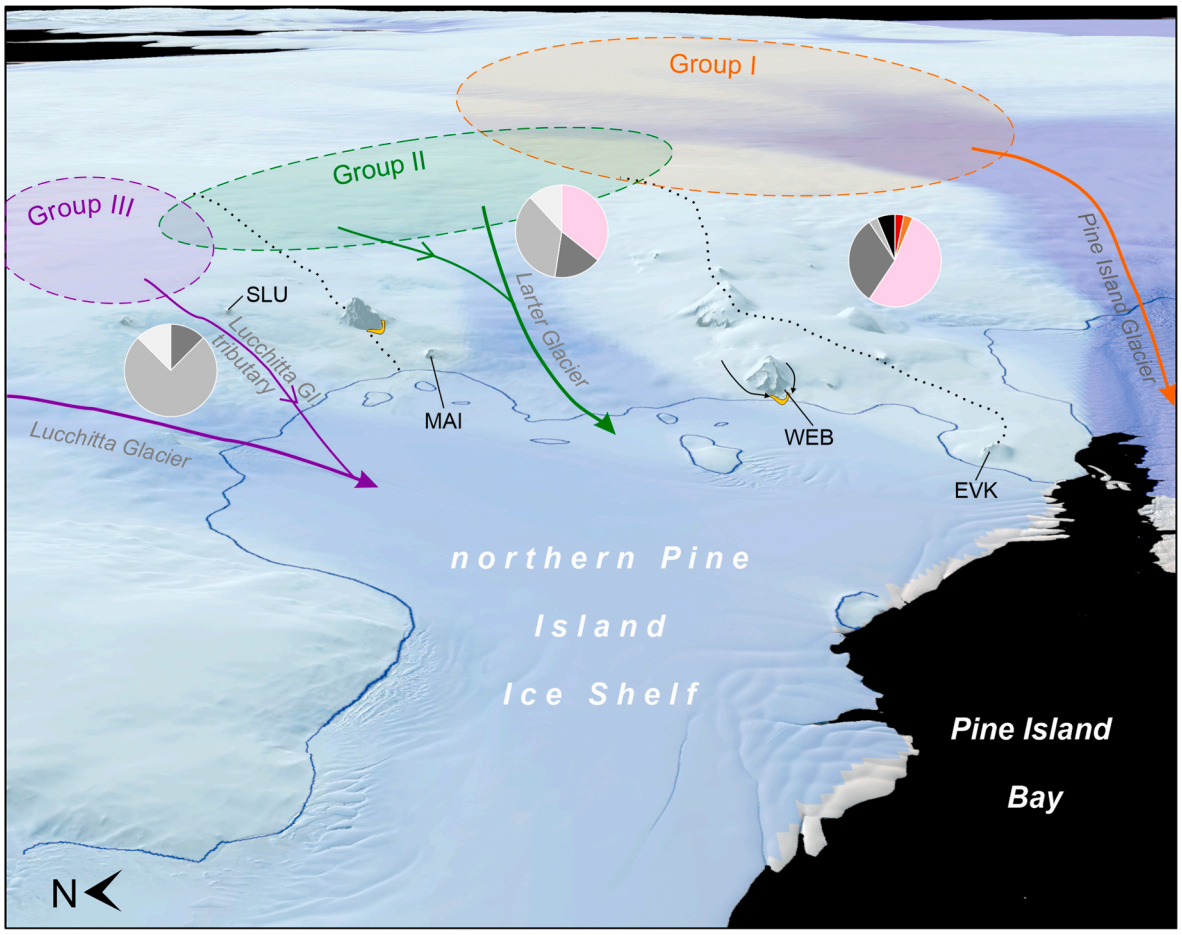

Fig. 11. Schematic illustration of possible former ice flow pathways in the Hudson Mountains, deduced from the distribution and lithology of erratic cobbles deposited on the nunataks. Pathways for PIG, Larter and Lucchitta glaciers are shown with orange, green and purple arrows respectively, with accompanying pie charts (also shown in Fig. 4) to show the proportions of erratic lithologies deposited on the nunataks associated with each glacier. The ice divides separating each drainage basin are shown as dotted black lines. The ovals indicate possible extent and overlap of source areas for erratics in each group. The yellow areas at Webber Nunatak and Mount Moses indicate presence of moraine. Selected nunataks are labelled to help with orientation: SLU=Slusher Nunatak, MAI=Maish Nunatak, WEB=Webber Nunatak, EVK=Evans Knoll. The satellite image is Landsat-9 [acquired January 4, 2024], courtesy of the U.S. Geological Survey. In the background, the image fades to LIMA (Bindschadler et al., 2008). The scale varies across the image; for distances, refer to Fig. 1. The 2011 grounding lines (Rignot et al., 2016; Gerrish et al., 2024) are shown as solid blue lines. The ice velocity is from Rignot et al. (2017) and is shown with the same colour ramp/scale as in Figs. 1 and 2.

shaped and transported by a highly erosive warm-based ice sheet. This finding is consistent with existing ^{10}Be exposure age data from a subset of nunataks in the Hudson Mountains (Johnson et al., 2014; Nichols et al., 2023). Those data show no evidence for ^{10}Be inheritance from exposure prior to the last glacial period, implying that glacial transport must have been erosive enough to remove evidence of prior exposure.

- The similarity in degree of weathering of the erratics suggests that they were all deposited by one phase of glaciation, rather than during multiple glacial cycles. The complete absence of pre-LGM ^{10}Be exposure ages in the published dataset implies that the last ice cover of all the nunataks in the Hudson Mountains likely occurred during the last glacial period.
- The difference in lithology of erratics deposited on the southernmost nunataks adjacent to PIG — dominated by granites — and northernmost nunataks adjacent to a tributary of Lucchitta Glacier — dominated by granodiorites and tonalites — suggests that ice formerly flowing through/over the Hudson Mountains transported material eroded from at least two (as yet unidentified) upstream source regions. This finding further implies that the ice flowing over the Hudson Mountains was not a single ice stream but was already divided into at least two tributaries during the last glacial period.

CRediT authorship contribution statement

Joanne S. Johnson: Conceptualization, Methodology, Validation, Formal analysis, Investigation, Data curation, Writing – original draft, Visualization, Project administration. **Keir A. Nichols:** Visualization, Methodology, Writing – review & editing. **Teal R. Riley:** Investigation, Writing – review & editing. **Ryan A. Venturelli:** Resources, Writing – review & editing. **Dominic A. Hodgson:** Writing – review & editing. **Greg Balco:** Writing – review & editing. **Brenda Hall:** Writing – review & editing. **James A. Smith:** Investigation, Writing – review & editing. **John Woodward:** Investigation, Writing – review & editing.

Data availability

Location and geomorphological data for the erratics discussed in this study are provided as Supplementary Data (Tables S1 and S2) and are also publicly accessible in the UK Polar Data Centre (see Johnson, 2024; Johnson and Smith, 2024).

Declaration of competing interest

The authors declare that they have no known competing financial interests or personal relationships that could have appeared to influence

the work reported in this paper.

Acknowledgements

We are grateful for logistics support for the 2019/20 season from British Antarctic Survey (BAS) and the United States Antarctic Program, and for the 2010 season from the Captain, crew and Chief Scientist, Karsten Gohl, on cruise ANT-XXVI/3 of RV *Polarstern*. Thank you also to BAS Field Guides Tom King, Ashley Fusiarski, Ian McNab and Terry O'Donovan for their help in the field. We thank members of BAS's Mapping and Geographic Information Centre: Elena Field, Andrew Fleming, Louise Ireland and Nathan Fenney for providing topographic maps, GPS support/processing and sourcing satellite imagery for use during fieldwork, Laura Gerrish for help with Figs. 1, 2 and 11, and Aliaksandra Skachkova for making rose diagrams for Fig. 4. Discussions with Scott Braddock, Seth Campbell, Brent Goehring, Dylan Rood, Mike Bentley, Paul Carling, David Evans, Claus-Dieter Hillenbrand, Rob Larter, Steve Roberts, John Smellie and Robert Johnson helped in fieldwork planning and in shaping our interpretations. Geospatial support for this work was provided by the Polar Geospatial Center under NSF-OPP awards 1043681, 1559691, and 2129685. This work is part of the 'Geological History Constraints' project, a component of the International Thwaites Glacier Collaboration supported by grants by UK Natural Environment Research Council (NE/S006710/1, NE/S00663X/1, and NE/S006753/1) and US National Science Foundation (NSF-OPP 2317097) and is ITGC contribution #132. The LLNL contribution to this work was carried out under Contract DE-AC52-07NA27344. This is LLNL-JRNL-867352.

Appendix A. Supplementary data

Supplementary data to this article can be found online at https://doi.org/10.1016/j.quascirev.2024.109027.

Data availability

All data are publicly accessible in the UK Polar Data Centre (Johnson, 2024; Johnson and Smith, 2024).

References

Arndt, J.E., Larter, R.D., Friedl, P., Gohl, K., Höppner, K., Science Team of Expedition PS104, 2018. Bathymetric controls on calving processes at Pine Island Glacier. Cryosphere 12, 2039–2050. https://doi.org/10.5194/tc-12-2039-2018.

Balco, G., 2020. Technical note: a prototype transparent-middle-layer data management and analysis infrastructure for cosmogenic-nuclide exposure dating. Geochronology 2, 169–175. https://doi.org/10.5194/gchron-2-169-2020.

Banwell, A.F., Willis, I.C., Stevens, L.A., Dell, R.L., MacAyeal, D.R., 2024. Observed meltwater-induced flexure and fracture at a doline on George VI Ice Shelf, Antarctica. J. Glaciol. 1–14. https://doi.org/10.1017/jog.2024.31.

Benn, D.I., Ballantyne, C.K., 1993. The description and representation of particle shape. Earth Surf. Process. Landforms 18, 665–672. https://doi.org/10.1002/esp.3290180709.

Benn, D.I., Ballantyne, C.K., 1994. Reconstructing the transport history of glacigenic sediments: a new approach based on the co-variance of clast-form indices. Sediment. Geol. 91, 215–227. https://doi.org/10.1016/0037-0738(94)90130-9.

Bindschadler, R., Vornberger, P., Fleming, A.H., Fox, A.J., Mullins, J., Binnie, D., Paulsen, S.J., Granneman, B., Gorodetzky, D., 2008. The Landsat image mosaic of Antarctica. Rem. Sens. Environ. 112, 4214–4226. https://doi.org/10.1016/j.rse.2008.07.006.

Braddock, S., Hall, B.L., Johnson, J.S., Balco, G., Spoth, M., Whitehouse, P.L., Campbell, S., Goehring, B.M., Rood, D.H., Woodward, J., 2022. Relative sea-level data preclude major late Holocene ice-mass change in Pine Island Bay. Nat. Geosci. 15, 568–572. https://doi.org/10.1038/s41561-022-00961-y.

Brisbourne, A.M., Smith, A.M., Vaughan, D.G., King, E.C., Davies, D., Bingham, R.G., Smith, E.C., Nias, I.J., Rosier, S.H.R., 2017. Bed conditions of Pine Island Glacier, West Antarctica. J. Geophys. Res.-Earth 122, 419–433. https://doi.org/10.1002/2016JF004033.

Clark, P.U., Dyke, A.S., Shakun, J.D., Carlson, A.E., Clark, J., Wohlfarth, B., Mitrovica, J. X., Hostetler, S.W., McCabe, A.M., 2009. The last glacial maximum. Science 325 (5941), 710–714. https://doi.org/10.1126/science.1172873.

Evans, D.J.A., 2018. Till: A Glacial Process Sedimentology. Wiley & Sons, Chichester. https://doi.org/10.1002/9781118652541.

Fretwell, P., Pritchard, H.D., Vaughan, D.G., Bamber, J.L., Barrand, N.E., Bell, R., Bianchi, C., Bingham, R.G., Blankenship, D.D., Casassa, G., Catania, G., Callens, D., Conway, H., Cook, A.J., Corr, H.F.J., Damaske, D., Damm, V., Ferraccioli, F., Forsberg, R., Fujita, S., Gim, Y., Gogineni, P., Griggs, J.A., Hindmarsh, R.C.A., Holmlund, P., Holt, J.W., Jacobel, R.W., Jenkins, A., Jokat, W., Jordan, T., King, E. C., Kohler, J., Krabill, W., Riger-Kusk, M., Langley, K.A., Leitchenkov, G., Leuschen, C., Luyendyk, B.P., Matsuoka, K., Mouginot, J., Nitsche, F.O., Nogi, Y., Nost, O.A., Popov, S.V., Rignot, E., Rippin, D.M., Rivera, A., Roberts, J., Ross, N., Siegert, M.J., Smith, A.M., Steinhage, D., Studinger, M., Sun, B., Tinto, B.K., Welch, B.C., Wilson, D., Young, D.A., Xiangbin, C., Zirizzotti, A., 2013. Bedmap2: improved ice bed, surface and thickness datasets for Antarctica. Cryosphere 7, 375–393. https://doi.org/10.5194/tc-7-375-2013.

Gerrish, L., Ireland, L., Fretwell, P., Cooper, P., 2024. High resolution vector polylines of the Antarctic coastline (7.9). UK Polar Data Centre, Natural Environment Research Council, UK Research & Innovation. https://doi.org/10.5285/45c3cc90-098b-45e3-a809-16b80eed4ec2.

Graham, D.J., Midgley, N.G., 2000. Graphical representation of particle shape using triangular diagrams: an Excel spreadsheet method. Earth Surf. Process. Landforms 25, 1473–1477. https://doi.org/10.1002/1096-9837(200012)25:13<1473::AID-ESP158>3.0.CO;2-C.

Hodgson, D.A., Convey, P., Verleyen, E., Vyverman, W., McIntosh, W., Sands, C.J., Fernández-Carazo, R., Wilmotte, A., DeWever, A., Peeters, K., Tavernier, I., Willems, A., 2010. The limnology and biology of the Dufek Massif, Transantarctic Mountains 82° South. Polar Science 4, 197–214. https://doi.org/10.1016/j.polar.2010.04.003.

Hodgson, D.A., Bentley, M.J., 2013. Lake highstands in the Pensacola Mountains and Shackleton Range 4300–2250 cal. yr BP: evidence of a warm climate anomaly in the interior of Antarctica. The Holocene 23 (3), 388–397. https://doi.org/10.1177/0959683612460790.

Howat, I.M., Porter, C., Smith, B.E., Noh, M.-J., Morin, P., 2019. The reference elevation model of Antarctica. Cryosphere 13, 665–674. https://doi.org/10.5194/tc-13-665-2019.

Johnson, J., 2024. Orientations of bedrock striations in the Hudson Mountains, West Antarctica (Version 1.0). NERC EDS UK Polar Data Centre. https://doi.org/10.5285/7e80c81b-acc2-4a9b-9b5e-d37d49705524 [Data set].

Johnson, J.S., Bentley, M.J., Gohl, K., 2008. First exposure ages from the Amundsen Sea Embayment, West Antarctica: the Late Quaternary context for recent thinning of Pine Island, Smith, and Pope glaciers. Geology 36 (3), 223–226. https://doi.org/10.1130/G24207A.1.

Johnson, J.S., Bentley, M.J., Smith, J.A., Finkel, R.C., Rood, D.H., Gohl, K., Balco, G., Larter, R.D., Schaefer, J.M., 2014. Rapid thinning of Pine Island Glacier in the early Holocene. Science 343 (6174), 999–1001. https://doi.org/10.1126/science.1247385.

Johnson, J., Smith, J., 2024. Geomorphological measurements and lithological classifications of 90 erratic cobbles from the Hudson Mountains, West Antarctica (Version 1.0). NERC EDS UK Polar Data Centre. https://doi.org/10.5285/79c8eb39-5c19-440e-804f-816cd0b8e4bd [Data set].

Johnson, J.S., Smith, J.A., Schaefer, J.M., Young, N.E., Goehring, B.M., Hillenbrand, C. D., Lamp, J.L., Finkel, R.C., Gohl, K., 2017. The last glaciation of Bear Peninsula, central Amundsen Sea Embayment of Antarctica: constraints on timing and duration revealed by *in situ* cosmogenic ^{14}C and ^{10}Be dating. Quat. Sci. Rev. 178, 77–88. https://doi.org/10.1016/j.quascirev.2017.11.003.

Johnson, J.S., Pollard, D., Whitehouse, P.L., Roberts, S.J., Rood, D.H., Schaefer, J.M., 2021. Comparing glacial-geological evidence and model simulations of ice sheet change since the last glacial period in the Amundsen Sea sector of Antarctica. J. Geophys. Res.-Earth 126, e2020JF005827. https://doi.org/10.1029/2020JF005827.

Johnson, J.S., Woodward, J., Nesbitt, I., Winter, K., Campbell, S., Nichols, K.A., Venturelli, R.A., Braddock, S., Goehring, B.M., Hall, B., Rood, D.H., Balco, G., 2024. Assessing suitability of sites near Pine Island Glacier for subglacial bedrock drilling aimed at detecting Holocene retreat-readvance. EGUsphere. https://doi.org/10.5194/egusphere-2024-1452 [preprint].

Jordan, T.A., Thompson, S., Kulessa, B., Ferraccioli, F., 2023. Geological sketch map and implications for ice flow of Thwaites Glacier, West Antarctica, from integrated aerogeophysical observations. Sci. Adv. 9, eadf2639. https://doi.org/10.1126/sciadv.adf2639.

Joughin, I., Shapero, D., Smith, B., Dutrieux, P., Barham, M., 2021. Ice-shelf retreat drives recent Pine Island Glacier speedup. Sci. Adv. 7, eabg3080. https://doi.org/10.1126/sciadv.abg3080.

Kipf, A., Mortimer, N., Werner, R., Gohl, K., van dem Bogaard, P., Hauff, F., Hoernle, K., 2012. Granitoids and dykes of the Pine Island Bay region, West Antarctica. Antarct. Sci. 24 (5), 473–484. https://doi.org/10.1017/S0954102012000259.

Larter, R.D., Anderson, J.B., Graham, A.G.C., Gohl, K., Hillenbrand, C.-D., Jakobsson, M., Johnson, J.S., Kuhn, G., Nitsche, F.O., Smith, J.A., Witus, A.E., Bentley, M.J., Dowdeswell, J.A., Ehrmann, W., Klages, J.P., Lindow, J., Ó Cofaigh, C., Spiegel, C., 2014. Reconstruction of changes in the Amundsen Sea and Bellingshausen Sea sector of the West Antarctic Ice Sheet since the Last Glacial Maximum. Quat. Sci. Rev. 100, 55–86. https://doi.org/10.1016/j.quascirev.2013.10.016.

Lindow, J., Castex, M., Wittmann, H., Johnson, J.S., Lisker, F., Gohl, K., 2014. Glacial retreat in the Amundsen Sea sector, West Antarctica – first cosmogenic evidence from central Pine Island Bay and the Kohler Range. Quat. Sci. Rev. 98, 166–173. https://doi.org/10.1016/j.quascirev.2014.05.010.

Lukas, S., Benn, D.I., Boston, C.M., Brook, M., Coray, S., Evans, D.J.A., Graf, A., Kellerer-Pirklbauer, A., Kirkbride, M.P., Krabbendam, M., Lovell, H., Machiedo, M., Mills, S. C., Nye, K., Reinardy, B.T.I., Ross, F.H., Signer, M., 2013. Clast shape analysis and clast transport paths in glacial environments: a critical review of methods and the

role of lithology. Earth Sci. Rev. 121, 96–116. https://doi.org/10.1016/j.earscirev.2013.02.005.
Lupachev, A.V., Abakumov, E.V., 2013. Soils of Marie Byrd Land, West Antarctica. Eurasian Soil Sci. 46 (10), 994–1006. https://doi.org/10.1134/S1064229313100049.
Marschalek, J., Thomson, S., Hillenbrand, C.D., Vermeesch, P., Siddoway, C., Carter, A., Nichols, K., Rood, D.H., Venturelli, R.A., Hammond, S.J., Wellner, J., van de Flierdt, T., 2024. Geological insights from the newly discovered granite of Sif Island between Thwaites and Pine Island glaciers. Antarct. Sci. https://doi.org/10.1017/S0954102023000287.
Moriwaki, K., Iwata, S., Matsuoka, N., Hasegawa, H., Hirakawa, K., 1994. Weathering stage as a relative age of till in the central Sør-Rondane. Proc. NIPR Symp. Antarct. Geosci. 7, 156–161.
Morlighem, M., Rignot, E., Binder, T., Blankenship, D., Drews, R., Eagles, G., Eisen, O., Ferraccioli, F., Forsberg, R., Fretwell, P., Goel, V., Greenbaum, J.S., Gudmundsson, H., Guo, J., Helm, V., Hofstede, C., Howat, I., Humbert, A., Jokat, W., Karlsson, N., Lee, W.S., Matsuoka, K., Millan, R., Mouginot, J., Paden, J., Pattyn, F., Roberts, J., Rosier, S., Ruppel, A., Seroussi, H., Smith, E.C., Steinhage, D., Sun, B., van den Broeke, M.R., van Ommen, T.S., van Wessem, M., Young, D.A., 2020. Deep glacial troughs and stabilizing ridges unveiled beneath the margins of the Antarctic ice sheet. Nat. Geosci. 13, 132–137. https://doi.org/10.1038/s41561-019-0510-8.
Mukasa, S.B., Dalziel, I.W., 2000. Marie Byrd Land, West Antarctica: evolution of Gondwana's Pacific margin constrained by zircon U-Pb geochronology and feldspar common-Pb isotopic compositions. Geol. Soc. Am. Bull. 112 (2), 611–627. https://doi.org/10.1130/0016-7606(2000)112%3C611:MBLWAE%3E2.0.CO.
Nichols, K.A., Rood, D.H., Venturelli, R.A., Balco, G., Adams, J., Guillaume, L., Campbell, S., Goehring, B.M., Hall, B.M., Wilcken, K., Woodward, J.W., Johnson, J. S., 2023. Offshore-onshore record of Last Glacial Maximum-to-present grounding line retreat at Pine Island Glacier. Geology 51 (11), 1033–1037. https://doi.org/10.1130/G51326.1.
Owen, L.A., Robinson, R., Benn, D.I., Finkel, R.C., Davis, N.K., Li, C., Putkonen, J., Li, D., Murray, A.S., 2009. Quaternary glaciation of Mount Everest. Quat. Sci. Rev. 28, 1412–1433. https://doi.org/10.1016/j.quascirev.2009.02.010.
Pankhurst, R.J., Weaver, S.D., Bradshaw, J.D., Storey, B.C., Ireland, T.R., 1998. Geochronology and geochemistry of pre-jurassic superterranes in Marie Byrd Land, Antarctica. J. Geophys. Res. 103 (B2), 2529–2547. https://doi.org/10.1029/97JB02605.
Powers, M.C., 1953. A new roundness scale for sedimentary particles. J. Sediment. Petrol. 23 (2), 117–119. https://doi.org/10.1306/d4269567-2b26-11d7-8648000102c1865d.
Rignot, E., Mouginot, J., Scheuchl, B., 2016. MEaSUREs Antarctic Grounding Line from Differential Satellite Radar Interferometry, Version 2. NASA National Snow and Ice Data Center Distributed Active Archive Center, Boulder, Colorado USA. https://doi.org/10.5067/IKBWW4RYHF1Q. (Accessed 16 May 2024).
Rignot, E., Mouginot, J., Scheuchl, B., 2017. MEaSUREs InSAR-Based Antarctica Ice Velocity Map, Version 2. NASA National Snow and Ice Data Center Distributed Active Archive Center, Boulder, Colorado USA. https://doi.org/10.5067/D7GK8F5J8M8R. (Accessed 16 May 2024).
Rignot, E., Mouginot, J., Scheuchl, B., van den Broeke, M., van Wessem, M.J., Morlighem, M., 2019. Four decades of Antarctic Ice Sheet mass balance from 1979–2017. P. Natl. Acad. Sci. USA 116 (4), 1095–1103. https://doi.org/10.1073/pnas.1812883116.
Rowley, P.D., Laudon, T.S., La Prade, K.E., LeMasurier, W.E., 1986. Hudson Mountains. In: LeMasurier, W.E., Thomson, J.W. (Eds.), Volcanoes of the Antarctic Plate & Southern Oceans 48, 289–293. Antarctic Research Series 48.
Scambos, T.A., Bell, R.E., Alley, R.B., Anandakrishnan, S., Bromwich, D.H., Brunt, K., Christianson, K., Creyts, T., Das, S.B., DeConto, R., Dutrieux, P., Fricker, H.A., Holland, D., MacGregor, J., Medley, B., Nicolas, J.P., Pollard, D., Siegfried, M.R., Smith, A.M., Steig, E.J., Trusel, L.D., Vaughan, D.G., Yager, P.L., 2017. How much, how fast?: a science review and outlook for research on the instability of Antarctica's Thwaites Glacier in the 21st century. Global Planet. Change 153, 16–34. https://doi.org/10.1016/j.gloplacha.2017.04.008.
Schaefer, initial unknown, 1968. Field notes from Hudson Mountains survey, part of the US Ellsworth Land Survey, 1967-1968. the Polar Rock Repository, Byrd Polar and Climate Research Center. Ohio State University, USA. https://prr.osu.edu/. (Accessed 26 May 2023).
Simões Pereira, P., van de Flierdt, T., Hemming, S.R., Frederichs, T., Hammon, S.J., Brachfeld, S., Doherty, C., Kuhn, G., Smith, J.A., Klages, J.P., Hillenbrand, C.-D., 2020. The geochemical and mineralogical fingerprint of West Antarctica's weak underbelly: Pine Island and Thwaites glaciers. Chem. Geol. 550, 119649. https://doi.org/10.1016/j.chemgeo.2020.119649.
Smith, B., Fricker, H.A., Gardner, A.S., Medley, B., Nilsson, J., Paolo, F.S., Holschuh, N., Adusumilli, S., Brunt, K., Csatho, B., Harbeck, K., Markus, T., Neumann, T., Siegfried, M.R., Zwally, H.J., 2020. Pervasive ice sheet mass loss reflects competing ocean and atmosphere processes. Science 368 (6496), 1239–1242. https://doi.org/10.1126/science.aaz5845.
Sneed, E.D., Folk, R.L., 1958. Pebbles in the lower Colorado River, Texas, a study in particle morphogenesis. J. Geology 66, 114–150. https://doi.org/10.1086/626490.
Stone, J.O., Balco, G.A., Sugden, D.E., Caffee, M.W., Sass, L.C., Cowdery, S.G., Siddoway, C., 2003. Holocene deglaciation of Marie Byrd Land, West Antarctica. Science 299 (5603), 99–102. https://doi.org/10.1126/science.1077998.
Streickheisen, A., 1976. To each plutonic rock its proper name. Earth Sci. Rev. 12, 1–33. https://doi.org/10.1016/0012-8252(76)90052-0.
Sugden, D.E., Balco, G., Cowdery, S.G., Stone, J.O., Sass, L.C., 2005. Selective glacial erosion and weathering zones in the coastal mountains of Marie Byrd Land, Antarctica. Geomorphology 67, 317–334. https://doi.org/10.1016/j.geomorph.2004.10.007.
Thomas, R.H., Bentley, C.R., 1978. A model for Holocene retreat of the West Antarctic Ice Sheet. Quat. Res. 10 (2), 150—170. https://doi.org/10.1016/0033-5894(78)90098-4.
Wade, F.A., Craddock, C., 1969. Geology of the King Peninsula, Canisteo Peninsula and Hudson Mountains areas, Ellsworth Land, Antarctica. Antarct. J. U. S. 4 (4), 92.
Warner, R.C., Fricker, H.A., Adusumilli, S., Arndt, P., Kingslake, J., Spergel, J.J., 2021. Rapid formation of an ice doline on Amery Ice Shelf, East Antarctica. Geophys. Res. Lett. 48, e2020GL091095. https://doi.org/10.1029/2020GL091095.
Weertman, J., 1974. Stability of the junction of an ice sheet and an ice shelf. J. Glaciol. 13 (67), 3–11. https://doi.org/10.3189/S0022143000023327.
Werner, R., Daniel, K., Hauff, F., Veit, A., 2007. Composition and evolution of Cenozoic volcanic complexes and the crystalline basement of Marie Byrd Land and Ellsworth Land. In: Gohl, K. (Ed.), The Expedition ANTARKTIS-XXIII/4 of the Research Vessel "Polarstern" in 2006, vol. 557. Berichte zur Polar-und Meeresforschung, pp. 67–76. https://doi.org/10.2312/BzPM_0557_2007.
White, D., Bennike, O., Harley, S., Fink, D., Kiernan, K., McConnell, A., Wagner, B., 2009. Geomorphology and glacial history of the Rauer Group, East Antarctica. Quat. Res. 72, 80–90. https://doi.org/10.1016/j.yqres.2009.04.001.